
BAYESIAN SPATIOTEMPORAL NONSTATIONARY MODEL QUANTIFIES ROBUST INCREASES IN DAILY EXTREME RAINFALL ACROSS THE WESTERN GULF COAST

Yuchen Lu^{*†}, Benjamin Seiyon Lee², and James Doss-Gollin^{1,3}

¹Department of Civil and Environmental Engineering, Rice University, Houston, TX 77005

²Department of Statistics, George Mason University, Fairfax, Virginia 22030

³Ken Kennedy Institute, Rice University, Houston, TX 77005

^{*}yl238@rice.edu

February 5, 2025

ABSTRACT

Precipitation exceedance probabilities are widely used in engineering design, risk assessment, and floodplain management. While common approaches like NOAA Atlas 14 assume that extreme precipitation characteristics are stationary over time, this assumption may underestimate current and future hazards due to anthropogenic climate change. However, the incorporation of nonstationarity in statistical modeling of extreme precipitation has faced practical challenges which have restricted its applications. In particular, random sampling variability challenges the reliable estimation of trends and parameters, especially when observational records are limited. To address this methodological gap, we propose the Spatially Varying Covariates Model, a hierarchical Bayesian spatial framework that integrates nonstationarity and regionalization for robust frequency analysis of extreme precipitation. This model draws from extreme value theory, spatial statistics, and Bayesian statistics, and is validated through cross-validation and multiple performance metrics. Applying this framework to a case study of daily rainfall in the Western Gulf Coast, we identify robustly increasing trends in extreme precipitation intensity and variability throughout the study area, with notable spatial heterogeneity. This flexible model accommodates stations with varying observation records, yields smooth return level estimates, and can be straightforwardly adapted to analysis of precipitation frequencies at different durations and for other regions.

1 Introduction

Extreme precipitation poses risks to ecosystems, economies, and communities [Lall et al., 2018]. These risks are exacerbated by global warming and urbanization [Donat et al., 2016, Tedesco et al., 2020, Merz et al., 2014]. Notable recent examples illustrate the potential impacts of extreme precipitation. For example, in August 2017, Hurricane Harvey brought record-breaking rainfall that led to catastrophic flooding and damaged more than 150 000 homes in Southeast Texas [van Oldenborgh et al., 2017, Russell et al., 2020]. Similarly in July 2021, an extreme rainfall event struck Henan Province in China, resulting in 7.95 inch rainfall in an hour, a record in Zhengzhou, leading to hundreds of fatalities and billions of dollars in direct losses [Sun et al., 2023, Luo et al., 2023]. Moreover, less extreme localized heavy rainfall events can also cause localized flooding, disrupt transportation networks, and damage infrastructure, with large cumulative impacts in many urban areas [Moftakhari et al., 2018, Rosenzweig et al., 2018, Lopez-Cantu and Samaras, 2018]

To manage these risks, estimates of precipitation exceedance probabilities are widely used in engineering design, floodplain management, and policy analysis. These estimates are typically disseminated as Intensity-Duration-Frequency

^{*}Corresponding author

(IDF) curves, which describe the relationship between intensity, duration, and the probability of exceedance for rainfall at a single point in space [Martel et al., 2021, Gu et al., 2022]. For instance, IDF curves form the basis of synthetic design storms, which serve as inputs to hydrologic models for developing floodplain maps [The Federal Emergency Management Agency, 2019]. IDF curves are also used to manage less extreme floods, for example to size pipes used for site-scale stormwater management [Cook et al., 2020, Sharma et al., 2021]. In the United States, the National Oceanographic and Atmospheric Administration (NOAA) develops Atlas 14, a widely used set of IDF curves interpolated across space, and similar efforts exist in other regions [Silva et al., 2021, Kourtis and Tshirintzis, 2022, Haruna et al., 2023].

A key assumption underpinning most IDF curves in use today is that extreme precipitation characteristics are stationary over time, which means that the probability distribution of extreme precipitation does not change over time [Perica et al., 2013, 2018]. However, anthropogenic climate change and natural climate variability drive changes in the frequency, magnitude and spatiotemporal characteristics of heavy precipitation on multiple timescales [Milly et al., 2008, Pendergrass et al., 2017, Seneviratne et al., 2021, Sun et al., 2021]. Climate change contributes to extreme precipitation through both thermodynamic and dynamic changes [O’Gorman, 2015]. First-order thermodynamic responses are well-understood: following the Clausius-Clapeyron (C-C) relation, a warmer atmosphere holds more water, which can lead to increased rainfall. Dynamical changes are related to changes in weather patterns, and are more uncertain given the greater differences across different mechanisms and regions. These dynamical changes could amplify precipitation beyond what the C-C scaling rate predict, or could lead to less extreme precipitation in some regions [van Oldenborgh et al., 2017, Risser and Wehner, 2017]. Furthermore, changes in land use and land cover could have an impact on not only the rainfall-runoff relationships but also the fine-scale characteristics of extreme precipitation [Pielke Sr. et al., 2007, Mahmood et al., 2014, Aich et al., 2024, Zhang et al., 2018, Sui et al., 2024].

Recognition of these factors has motivated numerous calls to advance beyond the stationarity assumption [Milly et al., 2008, Cheng and AghaKouchak, 2014]. Yet credibly and reliably incorporating nonstationarity into extreme precipitation probabilities remains a methodological challenge. Estimates of trends must come either from General Circulation Models (GCMs) or from observations, and both approaches have fundamental limitations. Methods based on GCMs must address challenges such as the coarse spatial and temporal resolution of GCM outputs, which require down-scaling and bias correction approaches that can introduce substantial error and uncertainty [Lafferty and Sriver, 2023, Ehret et al., 2012, Farnham et al., 2018, Cannon et al., 2015]. More critically, dynamical biases, whether stemming from inadequate sampling of global dynamics such as El Niño–Southern Oscillation (ENSO) [Feng et al., 2019], inaccuracies in simulating regional and local processes that govern processes such as tropical cyclone formation, growth, and steering [Sobel et al., 2023], or meridional biases in jet stream location [Farnham et al., 2018], substantially affect local hazard estimates. These biases are not easily addressed through post-processing and often result in high uncertainty both within and across models and methods [Lafferty and Sriver, 2023, Dittes et al., 2018].

While observation-based approaches to trend estimation address many of these problems by relying on actual observations rather than on imperfect global models, short observational records and the rare nature of extreme events pose long-standing and well-recognized statistical challenges relating to sampling variability [Merz et al., 2014]. Various methodologies attempt to navigate these challenges in different ways, each with its strengths and limitations. One approach is to use a stationary model within a moving window, which allows for trends to be estimated implicitly without explicit parameterization. However, this approach exacerbates the problem of estimating the probability of rare events from short records [Doss-Gollin et al., 2019]. For example, Fagnant et al. [2020] apply a moving window estimator to rainfall probabilities on the Gulf Coast and find physically implausible discrepancies in trends and return level estimates between nearby locations as well as high volatility in return level estimates at a given location. Another approach is to model nonstationarity by conditioning the parameters of a statistical distribution on time-varying covariates, ideally credibly simulated by GCMs and having a physical relationship with local precipitation [van Oldenborgh et al., 2017, Russell et al., 2020]. While commonly applied to hydrologic analysis [Schlef et al., 2023], this “process-informed” nonstationary framework increases the number of parameters to estimate and thus exacerbates the problem of sampling variability intrinsic to precipitation frequency analysis [Montanari and Koutsoyiannis, 2014, Serrinaldi and Kilsby, 2015].

To mitigate sampling variability between nearby stations, information can be pooled across space in a technique known as regionalization. In essence, regionalization methods assume that rainfall observed at one location is representative of rainfall at nearby locations, and thus can compensate for stations with short records by combining records from multiple gauges. Physically, this can be interpreted as a form of spatial averaging analogous to stochastic storm transposition [Wright et al., 2020] and can reduce sampling variability related to the random spatial structure of precipitation in a given storm. Many regionalization methods have been proposed. Notably, Regional Frequency Analysis [Hosking, 1997] aggregates data within the defined homogeneous regions that share similar climate and hydrologic characteristics. Similarly, region-of-influence approaches [Burn, 1990] dynamically group each station with nearby stations based on similarity criteria, resulting in smooth transitions across regional boundaries. While these and

other regionalization methods have been widely used in the development of IDF curves [Perica et al., 2018, Fowler and Kilsby, 2003], many common implementations rely on L -moments, which are not well-suited for nonstationary analysis [Salas et al., 2018]. Other studies have employed a wide variety of alternatives, including spatial Bayesian hierarchical models [Davison et al., 2012, Cressie and Wikle, 2011, Lee and Haran, 2022, Wikle, 2019, Cooley et al., 2007], max-stable processes [Stephenson et al., 2016], and semi-Bayesian methods [Ossandón et al., 2021] to pool information across space.

1.1 Objectives

To integrate the concepts of nonstationarity and regionalization into a coherent statistical framework for precipitation frequency analysis, we propose the Spatially Varying Covariates Model. This hierarchical Bayesian spatial framework can be applied to stations with varying measurement periods and yields robust extreme precipitation probability estimates. We apply this framework to daily extreme precipitation on the Western Gulf Coast, but it can be readily applied to other hazards and regions. Our objective is to shed light on three key research questions:

1. Can a hierarchical Bayesian space-time model accurately estimate the parameters of nonstationary extreme value distributions at gauged and ungauged locations?
2. How do extreme precipitation probabilities vary across space and time?
3. How do rainfall probability estimates from stationary models compare to those from nonstationary models?

We proceed as follows. Section 2 provides methodological details on our model and a case study of daily rainfall probabilities on the Western Gulf Coast. Section 3 presents results for our Gulf Coast case study. A discussion of our findings in section 4 is followed by a brief summary in section 5.

2 Methodology

In this section, we iteratively introduce components of our proposed Spatially Varying Covariates Model. We begin by describing fundamental concepts in section 2.1 and introduce our case study in section 2.2. Next, we outline the three models we use for comparison in section 2.3, with the full Spatially Varying Covariates Model described in section 2.3.3. Finally, we describe the validation and estimation methods in section 2.4 and section 2.5, respectively.

2.1 Conceptual Framework

Here, we present key theoretical building blocks that we integrate to form our Spatially Varying Covariates Model.

2.1.1 Stationary Model

Precipitation frequency analysis relies on statistical extreme value theory to estimate the probability of extreme precipitation events [Coles, 2001]. In this work we model block maxima using the Generalized Extreme Value (GEV) distribution, based on theoretical justification and extensive testing [Coles, 2001, Cooley et al., 2007, Mishra and Singh, 2010, Perica et al., 2018], but our approach could be extended to other distributions or to peaks over threshold analysis.

A stationary extreme value model assumes that the data generating process is invariant over time. Under the stationary GEV model, the probability distribution of annual maximum precipitation y in year t at station s is given by:

$$y(s, t) \sim \text{GEV}(\mu(s), \sigma(s), \xi(s)) \quad (1)$$

where μ is the location parameter, σ (positive) is the scale parameter, and ξ is the shape parameter. Often a single station is analyzed, in which case the s may be dropped.

2.1.2 Nonstationary GEV Model

Nonstationary extreme value statistics extend the traditional stationary framework by allowing parameters to vary in time for each station. Most generally, we can write the nonstationary model as:

$$y(s, t) \sim \text{GEV}(\mu(s, t), \sigma(s, t), \xi(s, t)) \quad (2)$$

There are many ways to model nonstationarity [Salas et al., 2018, Schlef et al., 2023]. Here, we consider the process-informed approach, which conditions the GEV parameters on climate indices:

$$\theta(s, t) = \alpha(s) + \sum_i \beta_i(s) x_i(t) \quad (3)$$

for a generic nonstationary GEV parameter $\theta(s, t)$, $\alpha(s)$ represents the corresponding regression intercept, $x_i(t)$ is a time-varying climate covariate, and $\beta_i(s)$ is the associated regression coefficient. For GEV models, either the location, scale, or both parameters can be modeled as nonstationary as in eq. (3). Suitable covariates should be chosen based on a physical understanding of the data-generating process such that they are causally related to extreme precipitation in a given region and. If projections are desired, these covariates should also be credibly simulated by global climate models [Farnham et al., 2018]. As with the stationary framework, the s notation is often dropped when analyzing a single station.

2.1.3 Gaussian Process

Previous research employing the process-informed framework (section 2.1.2) to estimate nonstationary extreme precipitation probabilities has found large estimation uncertainty [Cheng and AghaKouchak, 2014, Cooley and Sain, 2010] and implausibly large spatial variability when analyzing single stations [Fagnant et al., 2020]. In widely used IDF curves such as NOAA Atlas 14, this is addressed through smoothing as a post-processing step [Perica et al., 2018].

To mitigate the parametric uncertainty stemming from the increasing number of parameters and limited observation data, regionalization techniques that pool information across locations are commonly applied. Methods such as Regional Frequency Analysis and region-of-influence rely on defining homogeneous regions or grouping stations based on similarity, and typically use the L -moments method. Alternatively, some research use spatial Bayesian hierarchical frameworks, treating parameters as latent functions of space [Lee and Haran, 2022, Ulrich et al., 2020, Cooley et al., 2007]. These frameworks eliminate the need for multi-step processes like defining regions and offer flexibility to incorporate covariates.

To capture spatial dependencies, we incorporate a latent Gaussian Process (GP) layer to model the spatially varying distribution parameters. GPs are non-parametric models, providing full probability distributions not limited to point estimates [Rasmussen and Williams, 2006]. An advantage of this method is that we learn the spatial dependencies directly from the data, avoiding the need to define homogeneous clusters *a priori*. Using this method, the spatially varying distribution parameters can be estimated at all gauged stations and interpolated to ungauged locations, enabling the generation of gridded estimates from gauge points. GPs model the joint distribution of parameters at multiple locations using a multivariate normal distribution with a mean function and a kernel function:

$$f(x) \sim \mathcal{GP}(m(x), K(x, x')) \quad (4)$$

where $m(x)$ is the mean function and $K(x, x')$ is the kernel function that characterizes the similarity between two locations. We employ a constant mean function $m(x) = c$. Following some experimentation, we employ the exponential kernel, which has been widely used in previous research [Cooley et al., 2007, Ossandón et al., 2021] and has desirable convergence properties [Rasmussen and Williams, 2006, Cooley et al., 2007]. The exponential kernel is given by:

$$K(x_i, x_j) = \alpha^2 \exp\left(\frac{-|x_i - x_j|}{\rho}\right) \quad (5)$$

where $|x_i - x_j|$ is the euclidean distance between two locations, $\alpha > 0$ is the kernel variance, and $\rho > 0$ is the kernel length parameter. Alternative kernels may be considered in future work.

The posterior distributions of parameters are correlated, such that changes in one parameter would influence the values of others. In this research, we adopt univariate GPs to model the spatially varying parameters, which generates stable estimates without specifically enforcing correlations. Future work could explore methods like co-regionalization to account for this correlation [Gelfand et al., 2005, Schmidt and Gelfand, 2003].

2.2 Case Study

Our framework can be applied to extreme value analysis of any climate variable, but we focus on daily rainfall in the Western Gulf Coast region. Adjacent to the Gulf of Mexico, this area has experienced a substantial number of heavy rainfall and flooding events in the recent past. For instance, Harris County experienced the Memorial Day flood in 2015, when Brays Bayou received approximately 11 inch of rain in 12 hours [Bass et al., 2017]. Similarly, Hurricane Harvey in 2017 dropped more than 47.2 inch rainfall over and around Houston in 6 days [Zhang et al., 2018]. New Orleans has also endured a number of extreme rainfall events, such as Hurricane Katrina, which brought 14 inch inches of rain in a single day in August 2005 [Kates et al., 2006]. In August 2016, another intense precipitation event led to a total of 25.5 inch over a 3-day period, resulting in severe flooding that impacted around 60 600 homes [van der Wiel et al., 2017].

We extract Annual Maxima Series (AMS) from the Global Historical Climatology Network (GHCN) daily dataset for selected stations. Our model accommodates stations with both short and long observation records, but here we retain

stations with more than 30 years of available data and at least 99% data coverage each year. This selection leaves us with 181 stations with observations ranging from 1889 to 2022. To ensure consistency with NOAA Atlas 14 and to facilitate comparison, we converted the constrained 1-day records to unconstrained 24-hour records by multiplying the raw intensity by 1.11 as in NOAA Atlas 14 [Perica et al., 2018].

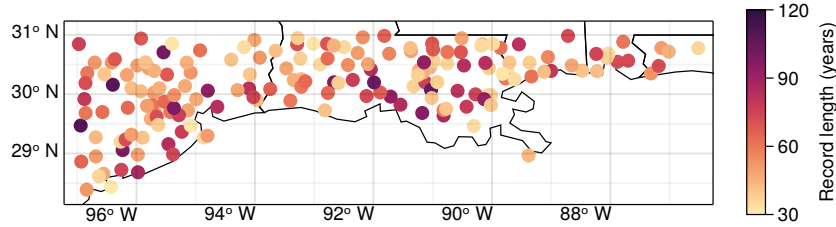


Figure 1: Figure shows the 181 selected stations from GHCN daily dataset. The colors indicate the number of available years, ranging from a minimum of 30 years to a maximum of approximately 120 years.

2.3 Proposed Framework

We propose the Spatially Varying Covariate Model (section 2.3.3), a fully probabilistic hierarchical spatial Bayesian framework that integrates nonstationarity and regionalization, to analyze the temporal trends of daily extreme precipitation in the Western Gulf Coast. This model integrates the concepts outlined in sections 2.1.1 to 2.1.3. To compare the performance of our proposed framework, we also apply two benchmark models to analyze the study area: the Pooled Stationary Model (section 2.3.1) and the Nonpooled Nonstationary Model (section 2.3.2).

2.3.1 Pooled Stationary Model

The **Pooled Stationary Model** incorporates regionalization within a stationary framework, conceptually similar to the method used in NOAA Atlas 14 [Perica et al., 2013, 2018]. In this model, we assume that the GEV parameters are constant over time (eq. (1)), with the location and scale parameters spatially pooled using univariate GPs. To ensure positivity, scale parameters are log-transformed. Given the relatively small size of the chosen study area, which primarily consists of coastal regions with little elevation variation, shape parameters are set as constant for all stations in this study [Cooley et al., 2007, Apputhurai and Stephenson, 2013]. For a larger study area encompassing diverse climate and topographic conditions, varying shape parameters is likely to be more advantageous.

For the GPs representing the spatially varying parameters (namely, the GEV location and scale parameters), we employ *Inverse Gamma* and *Gamma* distributions as the prior distributions for kernel variance (α_k) and length (ρ_k) parameters respectively, as they are strictly positive, as recommended by the Stan manual [Carpenter et al., 2017, Stan Development Team, 2022]. Priors of these two kernel parameters for both location and scale parameters follow Equations (22) and (23). For simplicity, we fix the GP mean (m_k) at 0, which does not substantially impact the final estimates. The prior for the shape parameter is informed by existing literature [Lima et al., 2016] and preliminary single station analysis, with absolute values typically below 0.5. Additionally, in anticipation of a positively skewed distribution for extreme precipitation events, we enforce a positive shape parameter [Blanchet et al., 2016, Ansh Srivastava and Mascaro, 2023]. The model is thus given as follows, and the detailed priors are shown in section 2.3.3.

$$y(s, t) \sim \text{GEV}(\mu(s), \sigma(s), \xi) \quad (6)$$

$$\mu(s) \sim \text{GP}(0, K_\mu(s, s')) \quad (7)$$

$$\sigma(s) \sim \text{GP}(0, K_\sigma(s, s')) \quad (8)$$

2.3.2 Nonpooled Nonstationary Model

To benchmark the extent to which spatial pooling improves the performance of our proposed model, we introduce the **Nonpooled Nonstationary Model**, in which we conduct a process-informed nonstationary analysis for each station separately.

Previous studies in this region have used various climate predictors within the process-informed nonstationary frameworks. These include thermodynamic covariates related to temperature changes such as global or regional temperature [van Oldenborgh et al., 2017, Russell et al., 2020], dynamic changes related covariates like Niño 3.4 index [Risser and

Wehner, 2017], and climate forcing factors, particularly CO₂ concentrations [Risser and Wehner, 2017, Nielsen-Gammon, 2020].

In this study, we utilize global average CO₂ concentration as the climate covariate, serving as a proxy for long-term global warming while minimizing noise from natural variability and volcanic eruptions [Jorgensen and Nielsen-Gammon, 2024]. Since natural variability, like ENSO, is related to tropical cyclone events, eliminating this factor helps us distinguish the impacts attributed solely to anthropogenic climate change warming. We extract CO₂ data from two sources: monthly mean CO₂ measured at Mauna Loa Observatory [Keeling et al., 1976] dating back to 1958, and CO₂ records derived from ice cores at Law Dome [Rubino et al., 2019] from 1006 to 1978. CO₂ data from 1958 to 1978 are derived as the average of these two resources.

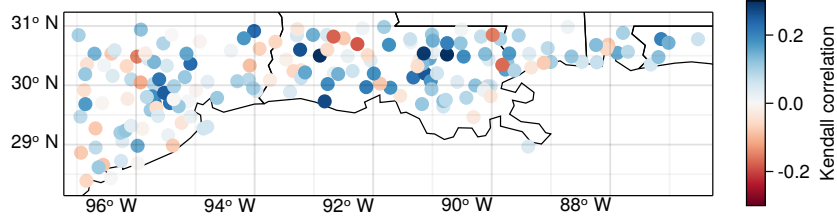


Figure 2: Annual maximum precipitation is positively correlated to $\ln \text{CO}_2$ at most stations. Each dot represents a station analyzed. Color indicates the rank correlation (Kendall's τ -b) between $\ln \text{CO}_2$ and annual maximum precipitation at each station. Blue (red) indicates positive (negative) relationships.

Specifically, we assume the GEV location and scale parameters are conditioned on $\ln \text{CO}_2$ (Equations (10) and (11)). Allowing location and scale parameters to vary simultaneously enables the distributions to both expand and shift to account for observed nonstationarity [Nielsen-Gammon, 2020]. Because shape parameters are hard to estimate, even in a stationary case [Coles, 2001], here we neglect temporal nonstationarity of shape parameters, consistent with the practices from some other previous research [Ragno et al., 2019, Song et al., 2020, Jorgensen and Nielsen-Gammon, 2024]. And we estimate the shape parameters at each station separately. Our model is thus given by:

$$y(s, t) \sim \text{GEV}(\mu(s, t), \sigma(s, t), \xi(s)) \quad (9)$$

$$\mu(s, t) = \alpha_\mu(s) + \beta_\mu(s)x(t) \quad (10)$$

$$\sigma(s, t) = \exp\{\log \alpha_\sigma(s) + \beta_\sigma(s)x(t)\} \quad (11)$$

$$\xi(s, t) = \xi \quad (12)$$

in which, α_μ and α_σ are the regression intercepts, β_μ and β_σ are the regression coefficients, and $x(t)$ is the time-varying climate covariate.

Within the Bayesian framework, we select priors based on general knowledge about the magnitude of extreme precipitation, avoiding strong priors that could overly bias the simulation results. For instance, daily AMS typically ranges from 2 inch to 20 inch, so we assign a Normal prior with a mean of 5 and a standard deviation of 5 to the location intercept. The prior for the shape parameter aligns with the stationary model (Equation (24)). Other remaining priors are set to be relatively uninformative. This yields a prior layer of:

$$\alpha_\mu \sim \text{Normal}(5, 5) \quad (13)$$

$$\log \alpha_\sigma \sim \text{Normal}(0, 1) \quad (14)$$

$$\beta_\mu \sim \text{Normal}(0, 1) \quad (15)$$

$$\beta_\sigma \sim \text{Normal}(0, 1) \quad (16)$$

Because estimation is conducted for each station separately, the prior is the same for each station considered, and there is no spatial layer.

2.3.3 Spatially Varying Covariates Model

The **Spatially Varying Covariates Model** extends on the benchmark models, combining spatial pooling and process-informed method to estimate robust daily extreme precipitation frequencies. Our final model is built upon the primary assumption that climate indices' impacts on heavy rainfall probabilities are spatially coherent, with nearby locations exhibiting similar spatiotemporal characteristics.

Explicitly, GEV location and scale parameters vary in space and time, and are represented with spatially varying parameters and time-varying variables. Similar to the benchmark models, shape parameter is assumed to be constant across time and space. In eqs. (10) and (11), we assume that the regression intercepts (μ_0 , $\log \sigma_0$) and coefficients (β_μ , β_σ) vary smoothly in space and are described with the latent GP layer (eqs. (18) to (21)).

For the Bayesian priors, kernel variance (α_k) and length (ρ_k) parameters for all the spatially varying parameters (in eqs. (10) and (11), μ_0 , $\log \sigma_0$, β_μ and β_σ) follow *Inverse Gamma* and *Gamma* distributions (eqs. (22) and (23)). We set the GP mean (m_k) as 0 as the Pooled Stationary Model. As a result, the parameter priors are set to match those used in the pooled stationary model and the nonpooled nonstationary model.

$$y(s, t) \sim \text{GEV}(\mu(s, t), \sigma(s, t), \xi) \quad (17)$$

$$\mu_0(s) \sim \text{GP}(0, K_{\mu_0}(s, s')) \quad (18)$$

$$\log \sigma_0(s) \sim \text{GP}(0, K_{\log \sigma_0}(s, s')) \quad (19)$$

$$\beta_\mu(s) \sim \text{GP}(0, K_{\beta_\mu}(s, s')) \quad (20)$$

$$\beta_\sigma(s) \sim \text{GP}(0, K_{\beta_\sigma}(s, s')) \quad (21)$$

$$\alpha_k \sim \text{InverseGamma}(5, 5) \quad (22)$$

$$\rho_k \sim \text{Gamma}(5, 1) \quad (23)$$

$$\xi \sim \text{Normal}(0, 0.5). \quad (24)$$

2.3.4 Experiment Design

We fit the three aforementioned frameworks to daily AMS data, evaluate their performance through cross-validation, and compare the heavy rainfall estimates with those from NOAA Atlas 14 [Perica et al., 2018]. Table 1 summarizes the similarities and differences between our three models with respect to key features. We further compare these three models to NOAA Atlas 14 for reference [Perica et al., 2018].

Table 1: Comparison of extreme precipitation analysis frameworks

	NOAA Atlas 14	Pooled Stationary	Nonpooled Nonstationary	Nonstationary	Spatially Varying Covariate
Stationarity	Stationary model	Stationary model	Process-informed nonstationary	Process-informed nonstationary	Process-informed nonstationary
Interpolation	Region of influence	Spatially pooled GEV	Each station separately	Each station separately	Spatially pooled climate impact parameters
Computation	L -moments	Bayesian	Bayesian	Bayesian	Bayesian

2.4 Validation

We conduct cross-validation in terms of time and space to evaluate the model performance.

First, to compare the three different frameworks outlined in section 2.3, we exclude observations from even (odd) years to assess the out-of-sample predictability on observations from odd (even) years. All stations are utilized to keep consistency since the Nonpooled Nonstationary Model simulates each station separately. To assess the out-of-sample predictive performance, we utilize the Logarithmic Score (LogS), Quantile Score (QS), and Continuous Ranked Probability Score (CRPS) to validate the probabilistic projections. For each validation metric, we first calculate the average across all simulated posterior distributions for a single observation, and then compute the average across all observation records.

Second, we conduct a spatial cross-validation of the Spatially Varying Covariates Model to assess how well the model is able to extrapolate to unobserved locations. Specifically, to avoid including nearby stations in the same subset, the study region is first partitioned into 25 grids (fig. A1). For each subset, five diagonal grids are excluded, and the model is fitted repeatedly to the remaining 20 grids of stations. Figure A2 shows the stations used to fit the model for the five subsets along with all available stations. The estimates for the excluded stations are compared with those obtained using all stations. This allows us to assess the model’s ability to extrapolate not only to unobserved locations, but also to stations without any nearby observations.

We use several validation scores to assess the model performance. LogS [Selten, 1998, Gelman et al., 2014] calculates the negative logarithm of the posterior predictive density. It assesses the overall likelihood of the observations given the simulated distributions, and lower LogS value is often desired. For an observation y_i at station s in year t given all the posterior simulations, the LogS is:

$$-\log p_{\text{post}}(y_i) = -\log \mathbb{E}_{\text{post}}(p(y_i|\theta)) = -\log \int p(y_i|\theta)p_{\text{post}}(\theta) d\theta \quad (25)$$

where $p_{\text{post}}(y_i)$ is the predictive density for observation y_i given the simulated posterior distributions, $\mathbb{E}_{\text{post}}(p(y_i|\theta))$ is the expected value of the likelihood $p(y_i|\theta)$ with respect to the posterior distribution parameters θ , $p_{\text{post}}(\theta)$ is the posterior distribution, and $\int p(y_i|\theta)p_{\text{post}}(\theta) d\theta$ is the average of likelihood given all posterior distributions.

The QS [Ulrich et al., 2020, Bentzien and Friederichs, 2014, Koenker and Machado, 1999] measures the weighted difference between observation and the modeled quantiles. It assesses how well the simulations match observations at different parts of the distribution, especially useful for extremes. Typically, a smaller QS value indicates a more reliable model. The quantile score for an observation y_i for a particular non-exceedance probability p is calculated:

$$QS(p) = \frac{1}{N} \sum_{n=1}^N \rho_p(y_i - q_{p,n}) \quad (26)$$

$$\rho_p(u) = \begin{cases} pu & \text{if } u > 0 \\ (p-1)u & \text{if } u \leq 0 \end{cases} \quad (27)$$

where N is the total number of simulations, $q_{p,n}$ is the corresponding modeled quantiles at probability p , and ρ_p is the loss function.

CRPS [Bröcker, 2012] quantifies the integrated squared difference between the predicted Cumulative Distribution Function (CDF) and the actual observation. It evaluates the overall accuracy of simulated distributions. CRPS close to 0 indicates better accuracy. It is given by:

$$\text{CRPS}(F, y_i) = \int_{-\infty}^{\infty} [F(x) - \mathbb{I}\{x \geq y_i\}]^2 dx \quad (28)$$

where F is the CDF of X , i.e. $F(x) = P[X \geq y]$; y_i is the observation; $\mathbb{I}(x)$ is 1 if the real argument is positive or zero, 0 otherwise.

2.5 Estimation

The field of hydrological frequency analysis has developed a wide range of methods for estimating model parameters. Traditionally, point estimators including methods of moments, Maximum Likelihood Estimation (MLE) [Martins and Stedinger, 2000, Stedinger, 1997], and L -moments have been widely used [Perica et al., 2018, Hosking, 1990, 1997]. However, moment-based methods have limited flexibility to be integrated with the process-informed framework [Cooley et al., 2007, Katz et al., 2002]. In contrast, Bayesian statistical analysis offers a more adaptable approach, enabling the incorporation of nonstationary and regionalization through a hierarchical Bayesian framework [Ragno et al., 2019, Thiemann et al., 2001]. This method provides interpretable probabilistic predictions by updating prior knowledge of unknown quantities using observational data. Specifically, the posterior probability is derived from the prior probability and the likelihood function [Gelman et al., 2014]. Additionally, Bayesian models can be effectively diagnosed with tools such as trace plots and Rhat values, ensuring model convergence and reliability [Gelman et al., 2020].

Given a model and data, we use Markov Chain Monte Carlo (MCMC) to estimate the posterior distribution of model parameters. To speed up convergence [Cooley et al., 2007], we set the initial values as the Maximum a posteriori (MAP) results. The Bayesian framework is built in R and the stan programming language, and we employ the No-U-Turn-Sampler (NUTS) simulator [Stan Development Team, 2022]. A total of 4 chains each of 10 000 samples are simulated, when the first half is set as the “warm-up” phase. Posterior GEV parameters are used to compute return levels for all MCMC simulations and are further analyzed to determine uncertainty ranges and expected estimates.

3 Results

We fit AMS of daily precipitation from the selected stations to each of the three models: Pooled Stationary Model, Nonpooled Nonstationary Model, and Spatially Varying Covariates Model. In section 3.1 we assess the performance of the Spatially Varying Covariates Model. In section 3.2 we show the spatial pattern of estimated model parameters, return level, and trends over time at each station. In section 3.3 we compare the Spatially Varying Covariates Model to the two alternatives and with NOAA Atlas 14 estimates.

3.1 Model performance

A critical question is whether our proposed model accurately and robustly captures nonstationary precipitation probabilities. We assess the performance of the Spatially Varying Covariates Model using three approaches. First, we use standard MCMC diagnostics to assess the convergence and sampling of our model [Gelman et al., 2020]. Figure A3 shows the trace plots of key distribution parameters, which appear to be qualitatively well-mixed. Additionally, \hat{R} values close to 1 are consistent with sufficient sampling and convergence [Gelman et al., 2014, chapter 11].

Next, we develop a graphical diagnostic to assess the quality of our fit. Tools like residual plots and quantile-quantile plots are widely used in regression and extreme value analysis to assess model fit. However, these tools are poorly suited for diagnosing nonstationary extreme value models across multiple locations. Our model is spatiotemporal, meaning that we estimate a unique GEV distribution for each station and year. For each observation, we compute the posterior probability of the observation given this posterior distribution. If our model is well-calibrated, samples should appear in the bottom tenth of their respective posterior distributions as frequently as they do in the top tenth. In other words, the observations should be uniformly distributed across all quantiles of the posterior distributions. Figure 3 shows the histogram of the posterior probability of the observations given the posterior GEV distributions. The histogram generally displays nearly uniform shape, suggesting that the model is well-calibrated, both for the overall distribution and especially for the upper tail.

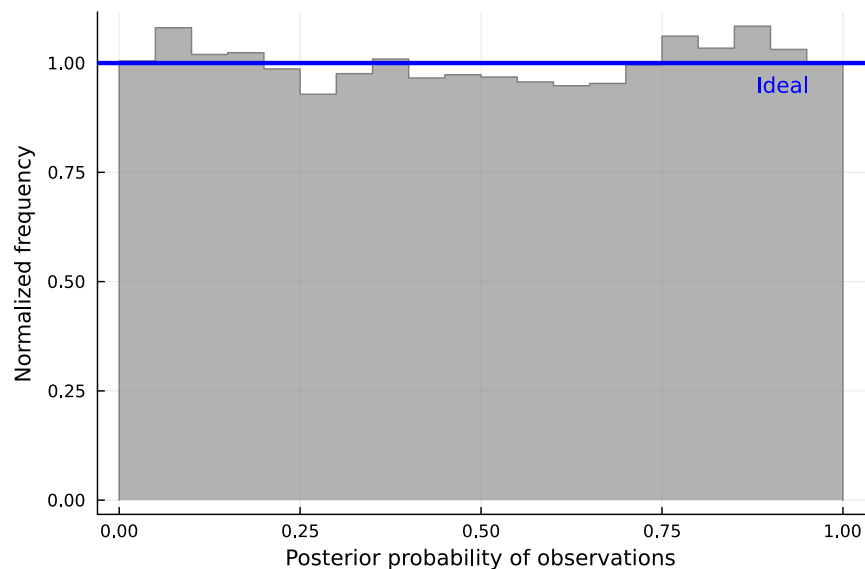


Figure 3: The observations are well-distributed across the quantiles of the posterior distributions, indicating that the Spatially Varying Covariates Model can effectively capture the variability in the observations. Histogram plot shows the posterior probability of observations given the posterior GEV distributions.

Third, we evaluate how well the Spatially Varying Covariates Model predicts out-of-sample heavy rainfall probabilities. To do this, we use $K = 5$ -fold cross-validation. First, we divide stations into five spatially structured subsets, as discussed in section 2.4 and illustrated in fig. A2. Then, we fit the model five times, leaving out one of the subsets each time, and then compare the estimates obtained from these subsets with those using all station observations.

Figure 4 compares the posterior distribution of 100-year return level when using the full model and out-of-sample estimates for ten representative stations (two from each of the five subsets). Although some differences between the posterior distributions are evident, as expected, the posterior means are very similar for most stations. Figure 5 presents the 100-year return level estimates (for 2022 CO_2 levels) for all stations, comparing simulations using all stations to those from the 5 subsets. Both the spatial patterns and the magnitude of return levels are generally consistent across the six (five subsets plus the full model) simulations. These findings support to the model’s ability to robustly predict nonstationary return levels at unobserved locations

3.2 Spatial and temporal patterns of daily extreme precipitation

A second key question is how the probabilities of extreme precipitation vary in space and time.

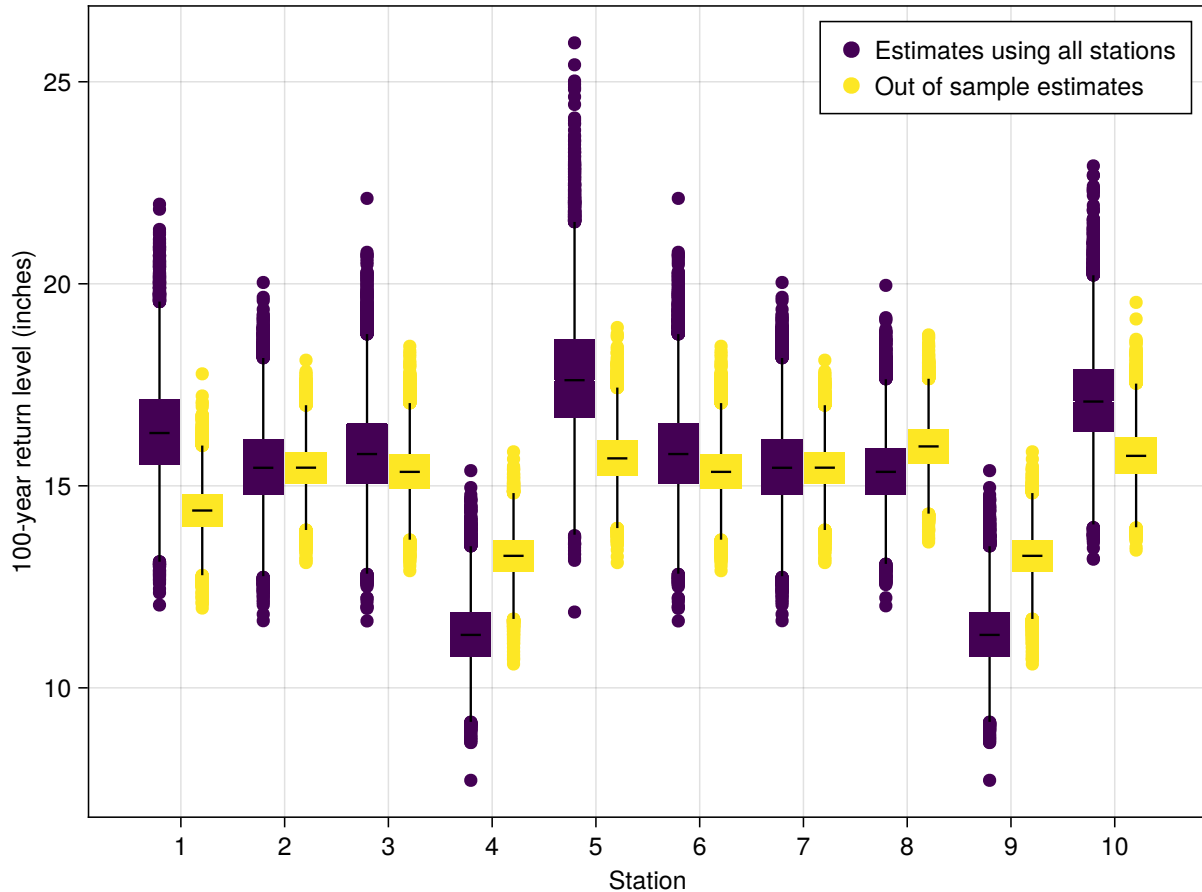


Figure 4: Out-of-sample probabilistic inferences generally agree with those from the full dataset. The plot shows posterior estimates of 100-year return level in 2022 when (dark) using all data (light) and using station subsets (out-of-sample). We choose to present results for 2 stations from each of the 5 subsets, representing different areas of the study region.

3.2.1 Robust nonstationary parameter estimates

We employ the process-informed nonstationary framework, wherein GEV location and scale parameters are treated as functions of global mean CO_2 . However, as discussed in section 1, a longstanding critique of nonstationary models is practical in nature, relating to the large estimation uncertainty associated with estimating more parameters from the same data [Serinaldi and Kilsby, 2015]. To assess whether the Spatially Varying Covariates Model can robustly estimate the nonstationary parameters, we compare the coefficients estimated from the Spatially Varying Covariates Model and the Nonpooled Nonstationary Model. As shown in fig. 6, the Nonpooled Nonstationary Model yields estimates that vary substantially even between nearby stations, similar to previous efforts [Fagnant et al., 2020]. In contrast, the Spatially Varying Covariates Model yields spatially smooth coefficient estimates. Across the majority of the study area, $\ln \text{CO}_2$ demonstrates a positive correlation with both GEV parameters. This indicates that as global CO_2 concentration rise, both the GEV location and scale parameters increase, indicating an increase in the overall intensity and variability in the extreme precipitation. The highest coefficient estimates are found around Houston and New Orleans, implying that these regions have the strongest increasing trends in extreme precipitation. It is worth noting that if we use a semi-Bayesian framework, where point estimates are developed separately at each station and then smoothed as in Ossandón et al. [2021], the coefficient estimates would differ significantly from those of our fully spatial model.

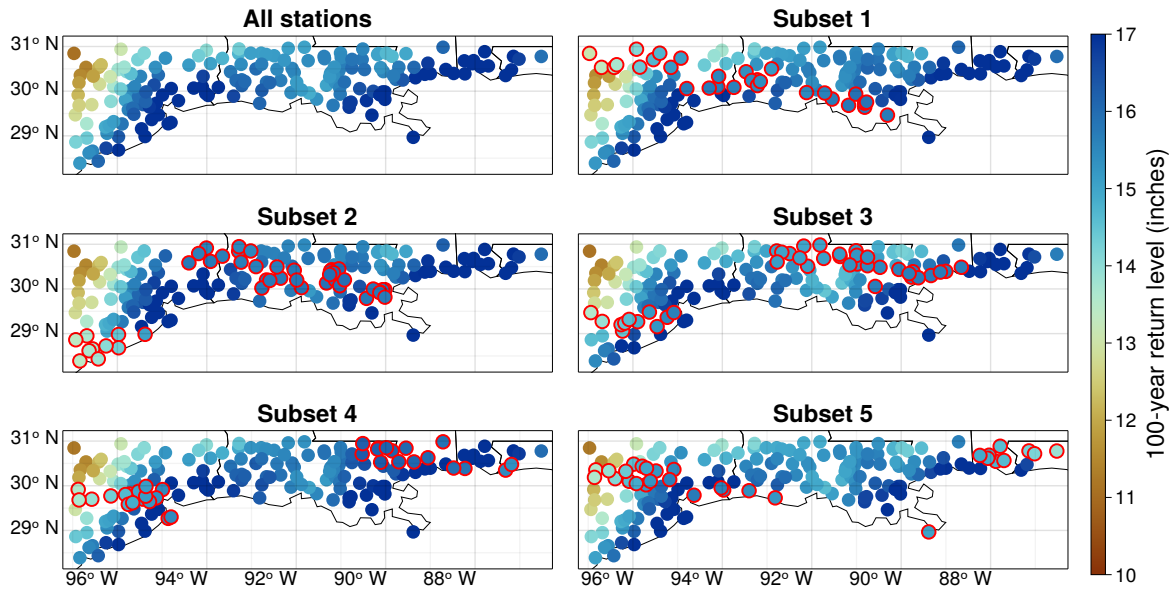


Figure 5: Out-of-sample estimates generally match estimates with full dataset. The maps present 100-year return level estimates at all stations when using all stations and station subsets. The circled stations are excluded for the specific station subset (out-of-sample).

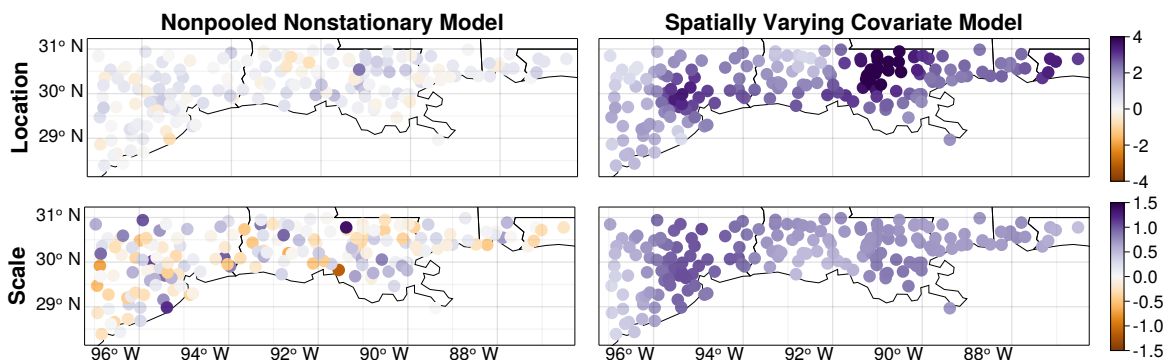


Figure 6: Climate change contributes to increases in intensity and variability of extreme precipitation. Figure shows the posterior mean of the coefficients of $\ln \text{CO}_2$ on (T) GEV location (β_μ in Equation (10)) and (B) GEV scale (β_σ in Equation (11)) parameters based on the (L) Nonpooled Nonstationary Model and (R) Spatially Varying Covariates Model.

3.2.2 Changes in return levels

Figure 6 indicates that both the location and scale parameters exhibit sensitivity to global CO_2 concentration. However, applications of precipitation extremes are often based on return levels, which are the expected value of the precipitation amount that is exceeded with a given probability. To analyze the spatiotemporal characteristics of extreme precipitation probabilities, we plot the return level estimates in 2022 and 1940, as well as the percentage change from 1940 to 2022 in fig. 7. We also generate gridded estimates by interpolating distribution parameters to grid center (section 2.1.3), shown in fig. A4. We find that return levels have increased by between 10 and 35% over the past 80 years throughout the study region, with the largest increases observed in coastal Southeast Texas and coastal southeastern Louisiana.

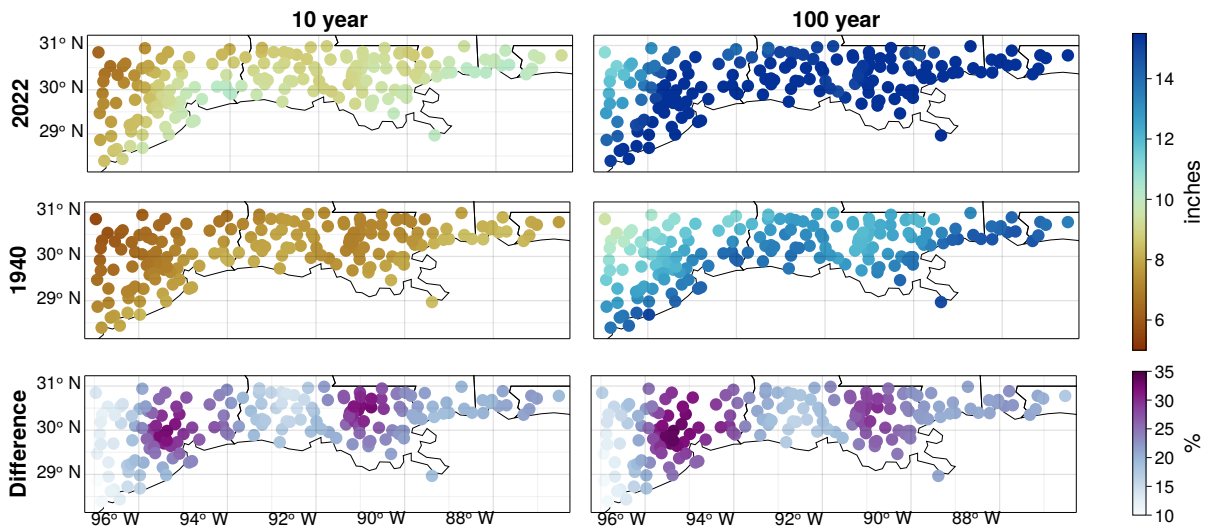


Figure 7: The Spatially Varying Covariates Model projects spatially consistent increases in daily heavy rainfall probabilities in the western Gulf Coast. These maps show the posterior mean of the (L) 10-year and (R) 100-year extreme precipitation return level estimates (T) in 2022 (M) in 1940 (B) percentage change from 1940 to 2022.

3.3 Model comparison

Another key question is how robust the Spatially Varying Covariates Model is compared to other frameworks that do not incorporate both nonstationarity and regionalization, and how the nonstationary extreme rainfall probability estimates compare to stationary estimates, such as those in NOAA Atlas 14.

3.3.1 Out-of-sample validations

To assess the out-of-sample predictability of the three frameworks (section 2.3), we carry out cross-validation by analyzing two subsets of the full data. Specifically, we model with odd (even) year observation records and validate the projections for the excluded even (odd) years with metrics outlined in section 2.4. Validation results are shown in table 2. Overall, the Spatially Varying Covariates Model performs similarly to the Pooled Stationary Model and is notably better than the Nonpooled Nonstationary Model.

LogS evaluates the probability of the observations based on the simulated posterior distributions. Since it measures negative log-likelihood, a lower LogS is desired, which indicates higher probability. The Pooled Stationary Model achieves the lowest LogS, suggesting that its predicted probabilities are most consistent with the observed AMS, and therefore provides a better match between the simulations and the actual observations. The Spatially Varying Covariates Model performs similarly well. However, the Nonpooled Nonstationary Model exhibits a significantly higher LogS. This model analyzes each station separately, and when half of the years are excluded, some stations are left with insufficient data (as few as 15 years of observations). This leads to high uncertainty in the estimates. Additionally, LogS heavily penalizes the unlikely events [Bjerregård et al., 2021]. As a result, the Nonpooled Nonstationary Model may generate distributions that predict some observations as extremely rare events, significantly increasing the LogS value.

QS measures how well the predicted quantiles match the observed values, and a smaller QS indicates better performance. Specifically, we evaluate extreme rainfall estimates with non-exceedance probabilities of 0.9, 0.98, 0.99 (corresponding to 10-, 50- and 100-year events). The two spatially pooled models show similar performance, with the Pooled Stationary Model achieving the lowest QS value at the non-exceedance probability of 0.9. The Spatially Varying Covariates Model, on the other hand, performs best at higher non-exceedance probabilities (0.98 and 0.99), indicating that this model better captures more extreme events. The Nonpooled Nonstationary Model yields the highest QS values, mainly due to the high uncertainties in the estimated quantiles.

CRPS provides a comprehensive assessment of simulation accuracy across all probabilities of the posterior distributions, with values close to 0 being preferred. In general, this metric favors models when observations are near the

median of the simulated distributions. Similar to LogS, the Pooled Stationary Model and the Spatially Varying Covariates Model show comparable CRPS values, though the former achieves slightly smaller values. These three metrics collectively indicate that the Spatially Varying Covariates Model outperforms the nonstationary framework at individual stations, while being comparable to the stationary framework. This suggests that integrating both nonstationary and regionalization could enhance nonstationary extreme precipitation analysis.

Table 2: Comparison of extreme precipitation analysis frameworks

	Pooled Stationary	Nonpooled Nonstationary	Spatially Varying Covariate
LogS	1.9322	1.9903	1.9495
QS ($p = 0.9$)	0.4671	0.5211	0.4712
QS ($p = 0.98$)	0.1689	0.2219	0.1680
QS ($p = 0.99$)	0.1027	0.1508	0.1018
CRPS	0.2548	0.2809	0.2574

3.3.2 Comparison with NOAA Atlas 14 estimates

Many practitioners will be interested in differences between our estimates and those from the current guidance. NOAA Atlas 14 utilizes historical observations until 2017 and adopts a stationary framework with regionalization. Figure 8 presents the percentage difference between the posterior mean return level estimates in 2022 from the three models and those from NOAA Atlas 14. In general, across these three frameworks, our estimates are higher than NOAA Atlas 14 estimates in the western part of the study area and lower in the eastern part. This spatial pattern in percentage differences is particularly pronounced for the Pooled Stationary Model and more extreme events, as shown for the 100-year events. Although both are stationary frameworks, differences in the regionalization method and data length contribute to this variation. The Nonpooled Nonstationary Model predominantly produces lower estimates for 10-year events but higher estimates for 100-year events. This indicates that nonstationarity could contribute to more extreme events. The Spatially Varying Covariates Model also tends to produce similar or lower estimates in the west, and higher estimates in the east, notably around western LA for 100-year events. The lower estimates around the Harris County region are consistent with some previous research [Nielsen-Gammon, 2020, Jorgensen and Nielsen-Gammon, 2024]. NOAA Atlas 14 utilizes observation data up to 2017, which is 5 years shorter than our analysis, and includes the occurrence of Hurricane Harvey in 2017. Stations with short observation records may overfit to the 2017 events, potentially resulting in events like Harvey being estimated as an event with a shorter return period.

We find that NOAA Atlas 14 underestimates return levels for 24-hour precipitation in New Orleans, Galveston, and Mobile under current conditions and overestimates return levels for 24-hour precipitation in Houston. However, the lower estimates in Houston do not imply that NOAA Atlas 14 is adequate for engineering design in the face of future climate change. Figure 9 depicts the time series of return level estimates from the Spatially Varying Covariates Model, projecting to 2050 using CO_2 concentrations from the Representative Concentration Pathway (RCP) 6 scenario. We project that under this scenario, NOAA Atlas 14 will underestimate return levels in Houston after around 2025.

4 Discussion

We contribute to a growing and multidisciplinary literature on links between extreme precipitation and climate. Methodologically, our reliance on observations to estimate nonstationary extreme precipitation draws primarily from engineering practice where accurate and local inferences are critical. Downscaled and bias-corrected rainfall data from GCMs offer broader spatial coverage and longer records, mitigating sampling variability in extreme rainfall probability estimates. However, inherent dynamical biases in GCMs limit their estimation reliability. Our findings of increasing extreme precipitation probabilities across the Gulf Coast from historical observations are consistent with previous studies [Fagnant et al., 2020, Jorgensen and Nielsen-Gammon, 2024, Statkewicz et al., 2021].

From a specific methodological perspective, the proposed Spatially Varying Covariates Model presents practical and theoretical advantages relative to other models for estimating nonstationary extreme precipitation probabilities from observations. Cheng and AghaKouchak [2014] examines nonstationary extreme rainfall probabilities at individual stations, highlighting the importance of incorporating climate change into design considerations. Ossandón et al. [2021] builds a process-informed GEV, estimating in a two-step framework: first, point estimates of the distribution parameters are developed for each station separately, and then these noisy estimates are smoothed and interpolated with a GP. While this approach improves scalability by enabling independent and parallel estimation at each station, it introduces additional bias and uncertainty by separately interpolating each parameter, disregarding the correlations

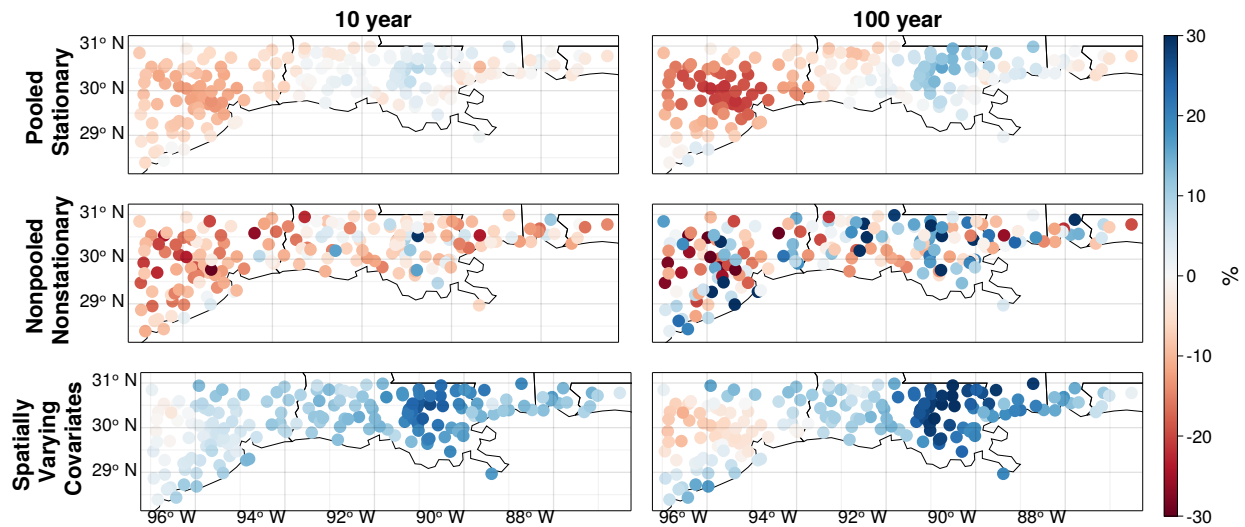


Figure 8: The Spatially Varying Covariates Model yields higher estimates in the eastern part of the study area and lower estimates in the western part compared to NOAA Atlas 14 estimates. The percentage difference between the estimates from NOAA Atlas 14 and our 2022 model implementation is illustrated as follows: (T) the Pooled Stationary Model, (M) Nonpooled Nonstationary Model, and (B) Spatially Varying Covariates Model for (L) 10-year and (R) 100-year events. Positive (blue) values indicate our estimates are higher, and negative (red) values indicate that our estimates are lower than NOAA Atlas 14 estimates. The percentage difference is calculated as: $(\text{our estimates in 2022} - \text{NOAA Atlas 14 estimates}) / \text{NOAA Atlas 14 estimates} * 100\%$.

between them. Alternatively, Dyrddal et al. [2015] develops a Bayesian hierarchical model, when the GEV parameters are regressed on spatial and temporal covariates. In this model, spatial coherence is achieved through the smoothness of the underlying spatial covariates. An advantage is that it may be easier to account for topographic features that cause stations that are nearby in longitude and latitude to have different GEV parameters. However, the choice of spatial covariates is challenging, as it's not immediately clear what the spatial covariates would be for a region like the Gulf Coast. Finally, Ulrich et al. [2020] employs a duration-dependent GEV distribution, modeling its parameters using polynomial basis functions within a stationary framework.

Several specific limitations of our model motivate further improvement and refinement. First, alternative distributions besides GEV distribution can be explored, such as the blended GEV [Castro-Camilo et al., 2022], which incorporates a GEV distribution with a 0 shape left tail and a positive shape right tail or the metastatistical distribution, which expands analysis beyond annual maxima [Miniussi and Marani, 2020]. Second, exploring how GP kernels beyond the exponential capture diverse data characteristics and improve the simulations. Third, improving estimation of parametric uncertainties. In our model, the observed annual maxima at two nearby locations is considered independent, conditional on the estimated parameters. However in reality, extreme events at adjacent locations are likely to be correlated. Max-stable process models seek to address this limitation, but are computationally demanding and difficult to implement [Stephenson et al., 2016]. Fourth, in regions with significant variations in topographic features, the inclusion of spatial variables such as elevation [Chu, 2012, Goovaerts, 2000, Hu et al., 2021, Talchabadel et al., 2018, Dyrddal et al., 2015] may enhance model performance. Fifth, one could extend our GP layer to account for the dependency among GEV parameters through a coregionalization approach [Gelfand et al., 2005, Schmidt and Gelfand, 2003]. Sixth, one could model uncertainty in observed precipitation or incorporate data from alternative sources such as remote sensing or radar data [Gavahi et al., 2023]. Finally, because our model requires estimating parameters at each station simultaneously, and because GPs estimation scales with the cube of the number of points, the computational complexity of our model may prove excessive for studies with many locations. In such cases, alternative spatial pooling methods like basis functions [Ramsay and Silverman, 2005] may offer computational efficiency while maintaining predictive quality.

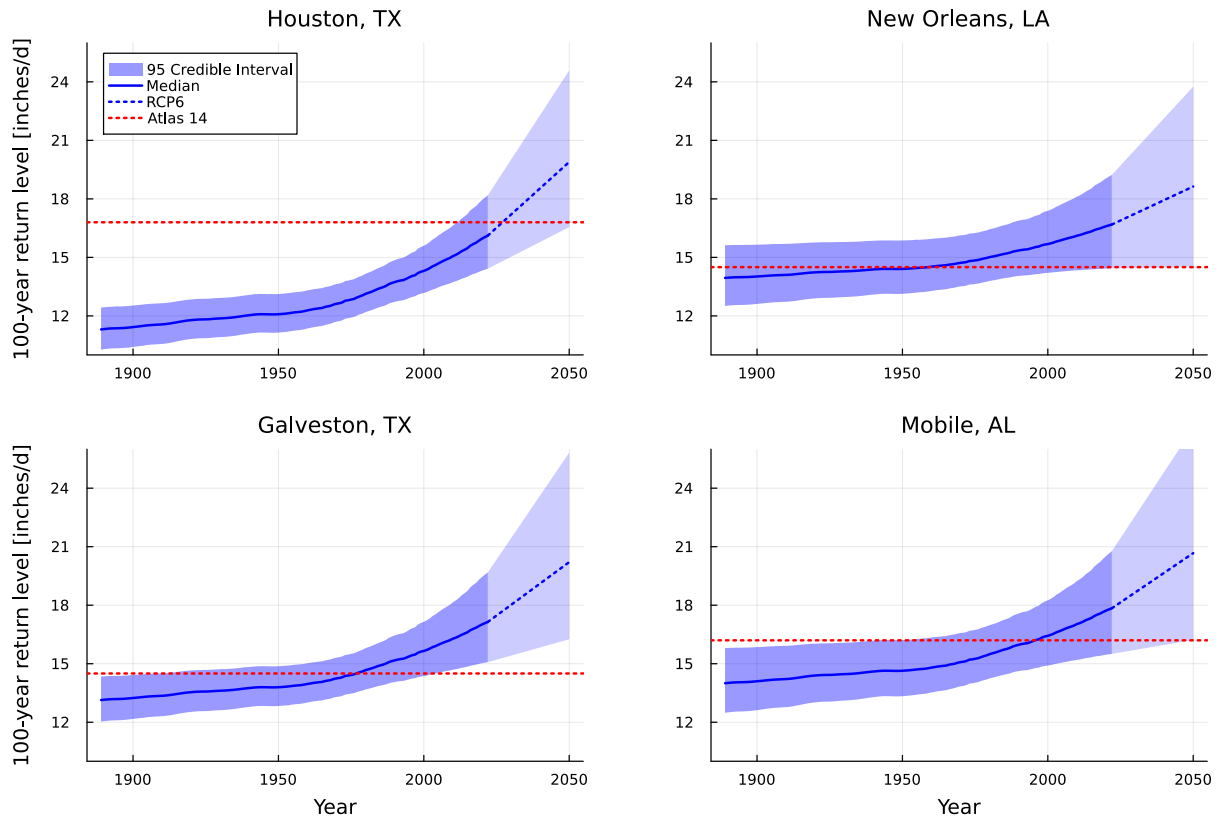


Figure 9: Future projections are higher than NOAA Atlas 14 estimates at major cities. Plots show the time series of 100-year return level for daily precipitation in selected cities estimated from the Spatially Varying Covariates Model compared to Atlas 14 guidelines. Dashed blue lines use CO_2 projections roughly corresponding to RCP 6. Blue shadows are the 95% credible interval from posterior estimates.

5 Conclusions

This study proposes a Bayesian hierarchical framework that integrates regionalization and nonstationarity to robustly estimate extreme precipitation probabilities. Using a case study that models annual maximum precipitation on the Western Gulf Coast with a GEV distribution, the Spatially Varying Covariates Model (1) introduces process-informed nonstationarity, meaning that parameters are conditioned on climate covariates, and (2) assumes that parameters vary smoothly across space. This framework naturally allows the use of gauges with incomplete observation records, pools information from nearby locations to generate smooth return level estimates, and can be applied to other regions, provided that suitable climate covariates are identified.

We demonstrate that the Spatially Varying Covariates Model provides robust estimates of return levels and their temporal trends. Through rigorous cross-validation, we show that our estimates are both well-calibrated and reliable. Specifically, the full model performs similarly to the stationary framework while outperforming the nonstationary framework at individual stations. Additionally, it generates reliable estimates at ungauged locations.

We find increase in 24-hour extreme rainfall across the study area, particularly in the areas surrounding Houston and New Orleans. Compared to the current guidance, Atlas 14, our estimates are generally lower in the western part and higher in the eastern part of the region. Future projections for 2050, based on GCMs, suggest that return levels will exceed Atlas 14 estimates at most locations, underscoring the inadequacy of current guidelines for engineering design under a changing climate.

Nonstationarity is widely recognized, but the statistical challenges of robustly estimating nonstationary extreme precipitation probabilities have largely motivated continued use of stationary models. This framework provides a practical and theoretically sound approach to estimating nonstationary extreme precipitation probabilities from observations.

Data Availability Statement

All data used in this research are publicly available. The daily rainfall data used to extract AMS records can be accessed from the GHCN at <https://www.ncei.noaa.gov/products/land-based-station/global-historical-climatology-network-daily>. The CO₂ data are sourced from Mauna Loa Observatory [Keeling et al., 1976] and Law Dome [Rubino et al., 2019], which are available at <https://gml.noaa.gov/ccgg/trends/data.html> and <https://data.csiro.au/collection/csiro%3A37077v3>, respectively. Code to implement the Spatially Varying Covariates Model and the other frameworks, as well as plotting results can be accessed at the following github repository: <https://github.com/yuchenluv/SpatiallyVaryingCovariateModel>.

Acknowledgments

This research was supported by Rice University and the Texas Water Development Board. The authors would like to thank Sylvia Dee, John Nielsen-Gammon, William Baule, Rewati Niraula, Saul Nuccitelli, and Srikanth Koka for insightful comments.

References

- Michael Aich, Philipp Hess, Baoxiang Pan, Sebastian Bathiany, Yu Huang, and Niklas Boers. Conditional diffusion models for downscaling & bias correction of Earth system model precipitation, April 2024.
- Nehal Ansh Srivastava and Giuseppe Mascaro. Improving the utility of weather radar for the spatial frequency analysis of extreme precipitation. *Journal of Hydrology*, 624:129902, September 2023. ISSN 0022-1694. doi: 10.1016/j.jhydrol.2023.129902.
- Pragalathan Apputhurai and Alec G. Stephenson. Spatiotemporal hierarchical modelling of extreme precipitation in Western Australia using anisotropic Gaussian random fields. *Environmental and Ecological Statistics*, 20(4): 667–677, December 2013. ISSN 1573-3009. doi: 10.1007/s10651-013-0240-9.
- Benjamin Bass, Andrew Juan, Avantika Gori, Zheng Fang, and Bedient Philip. 2015 Memorial Day Flood Impacts for Changing Watershed Conditions in Houston. *Natural Hazards Review*, 18(3):05016007, August 2017. doi: 10.1061/(asce)nh.1527-6996.0000241.
- Sabrina Bentzien and Petra Friederichs. Decomposition and graphical portrayal of the quantile score: Quantile Score Decomposition and Portrayal. *Quarterly Journal of the Royal Meteorological Society*, 140(683):1924–1934, July 2014. ISSN 00359009. doi: 10.1002/qj.2284.
- Mathias Blicher Bjerregård, Jan Kloppenborg Møller, and Henrik Madsen. An introduction to multivariate probabilistic forecast evaluation. *Energy and AI*, 4:100058, June 2021. ISSN 2666-5468. doi: 10.1016/j.egyai.2021.100058.
- J. Blanchet, D. Ceresetti, G. Molinié, and J.-D. Creutin. A regional GEV scale-invariant framework for Intensity–Duration–Frequency analysis. *Journal of Hydrology*, 540:82–95, September 2016. ISSN 00221694. doi: 10.1016/j.jhydrol.2016.06.007.
- Jochen Bröcker. Evaluating raw ensembles with the continuous ranked probability score. *Quarterly Journal of the Royal Meteorological Society*, 138(667):1611–1617, July 2012. ISSN 0035-9009, 1477-870X. doi: 10.1002/qj.1891.
- Donald H. Burn. Evaluation of regional flood frequency analysis with a region of influence approach. *Water Resources Research*, 26(10):2257–2265, 1990. ISSN 1944-7973. doi: 10.1029/WR026i010p02257.
- Alex J. Cannon, Stephen R. Sobie, and Trevor Q. Murdock. Bias Correction of GCM Precipitation by Quantile Mapping: How Well Do Methods Preserve Changes in Quantiles and Extremes? September 2015. doi: 10.1175/JCLI-D-14-00754.1.
- Bob Carpenter, Andrew Gelman, Matthew D Hoffman, Daniel Lee, Ben Goodrich, Michael Betancourt, Michael A Brubaker, Jiqiang Guo, Peter Li, and Allen Riddell. Stan: A probabilistic programming language. *Journal Of Statistical Software*, 76(1):1–29, January 2017. doi: 10.18637/jss.v076.i01.
- Daniela Castro-Camilo, Raphaël Huser, and Håvard Rue. Practical strategies for generalized extreme value-based regression models for extremes. *Environmetrics*, 33(6):e2742, September 2022. ISSN 1180-4009, 1099-095X. doi: 10.1002/env.2742.
- Linyin Cheng and Amir AghaKouchak. Nonstationary precipitation intensity-duration-frequency curves for infrastructure design in a changing climate. *Scientific Reports*, 4(1):7093, November 2014. ISSN 2045-2322. doi: 10.1038/srep07093.

- Hone-Jay Chu. Assessing the relationships between elevation and extreme precipitation with various durations in southern Taiwan using spatial regression models. *Hydrological Processes*, 26(21):3174–3181, October 2012. ISSN 0885-6087, 1099-1085. doi: 10.1002/hyp.8403.
- Stuart Coles. *An Introduction to Statistical Modeling of Extreme Values*. Springer Series in Statistics. Springer, London ;, 2001. ISBN 1-85233-459-2.
- Lauren M. Cook, Seth McGinnis, and Constantine Samaras. The effect of modeling choices on updating intensity-duration-frequency curves and stormwater infrastructure designs for climate change. *Climatic Change*, 159(2): 289–308, March 2020. ISSN 1573-1480. doi: 10.1007/s10584-019-02649-6.
- Daniel Cooley and Stephan R. Sain. Spatial hierarchical modeling of precipitation extremes from a regional climate model. *Journal of Agricultural, Biological, and Environmental Statistics*, 15(3):381–402, September 2010. ISSN 1537-2693. doi: 10.1007/s13253-010-0023-9.
- Daniel Cooley, Douglas Nychka, and Philippe Naveau. Bayesian spatial modeling of extreme precipitation return levels. *Journal of the American Statistical Association*, 102(479):824–840, September 2007. ISSN 0162-1459. doi: 10.1198/016214506000000780.
- Noel A. C. Cressie and Christopher K. Wikle. *Statistics for Spatio-Temporal Data*. Wiley, Hoboken, N.J., 2011. ISBN 978-0-471-69274-4.
- A. C. Davison, S. A. Padoan, and M. Ribatet. Statistical Modeling of Spatial Extremes. *Statistical Science*, 27(2), May 2012. ISSN 0883-4237. doi: 10.1214/11-STS376.
- Beatrice Dittes, Olga Špačková, Lukas Schoppa, and Daniel Straub. Managing uncertainty in flood protection planning with climate projections. *Hydrology and Earth System Sciences*, 22(4):2511–2526, 2018. doi: 10.5194/hess-22-2511-2018.
- Markus G. Donat, Andrew L. Lowry, Lisa V. Alexander, Paul A. O’Gorman, and Nicola Maher. More extreme precipitation in the world’s dry and wet regions. *Nature Climate Change*, 6(5):508–513, May 2016. ISSN 1758-6798. doi: 10.1038/nclimate2941.
- James Doss-Gollin, David J. Farnham, Scott Steinschneider, and Upmanu Lall. Robust adaptation to multiscale climate variability. *Earth’s Future*, 7(7):734–747, June 2019. ISSN 2328-4277. doi: 10.1029/2019ef001154.
- Anita Verpe Dyrørdal, Alex Lenkoski, Thordis L. Thorarinsdottir, and Frode Stordal. Bayesian hierarchical modeling of extreme hourly precipitation in Norway. *Environmetrics*, 26(2):89–106, 2015. ISSN 1099-095X. doi: 10.1002/env.2301.
- U Ehret, E Zehe, V Wulfmeyer, K Warrach-Sagi, and J Liebert. Should we apply bias correction to global and regional climate model data? *Hydrology and Earth System Sciences*, 16(9):3391–3404, 2012. doi: 10.5194/hess-16-3391-2012.
- Carlynn Fagnant, Avantika Gori, Antonia Sebastian, Philip B. Bedient, and Katherine B. Ensor. Characterizing spatiotemporal trends in extreme precipitation in Southeast Texas. *Natural Hazards*, 104(2):1597–1621, November 2020. ISSN 1573-0840. doi: 10.1007/s11069-020-04235-x.
- David J Farnham, James Doss-Gollin, and Upmanu Lall. Regional extreme precipitation events: Robust inference from credibly simulated GCM variables. *Water Resources Research*, 54(6), 2018. doi: 10.1002/2017wr021318.
- Jie Feng, Tao Lian, Jun Ying, Junde Li, and Gen Li. Do CMIP5 models show El Niño diversity? *Journal of Climate*, November 2019. ISSN 0894-8755. doi: 10.1175/jcli-d-18-0854.1.
- H. J. Fowler and C. G. Kilsby. A regional frequency analysis of United Kingdom extreme rainfall from 1961 to 2000. *International Journal of Climatology*, 23(11):1313–1334, 2003. ISSN 1097-0088. doi: 10.1002/joc.943.
- Keyhan Gavahi, Ehsan Foroumandi, and Hamid Moradkhani. A deep learning-based framework for multi-source precipitation fusion. *Remote Sensing of Environment*, 295:113723, September 2023. ISSN 0034-4257. doi: 10.1016/j.rse.2023.113723.
- Alan E. Gelfand, Sudipto Banerjee, and Dani Gamerman. Spatial process modelling for univariate and multivariate dynamic spatial data. *Environmetrics*, 16(5):465–479, August 2005. ISSN 1180-4009, 1099-095X. doi: 10.1002/env.715.
- Andrew Gelman, John B Carlin, Hal S Stern, and Donald B Rubin. *Bayesian Data Analysis*. Chapman & Hall/CRC Boca Raton, FL, USA, 3 edition, 2014.
- Andrew Gelman, Aki Vehtari, Daniel Simpson, Charles C. Margossian, Bob Carpenter, Yuling Yao, Lauren Kennedy, Jonah Gabry, Paul-Christian Bürkner, and Martin Modrák. Bayesian workflow. *arXiv:2011.01808 [stat]*, November 2020. doi: 10.48550/arXiv.2011.01808.

- P. Goovaerts. Geostatistical approaches for incorporating elevation into the spatial interpolation of rainfall. *Journal of Hydrology*, 228(1):113–129, February 2000. ISSN 0022-1694. doi: 10.1016/S0022-1694(00)00144-X.
- Xuezhi Gu, Lei Ye, Qian Xin, Chi Zhang, Fanzhang Zeng, Sofia D. Nerantzaki, and Simon Michael Papalexiou. Extreme Precipitation in China: A Review on Statistical Methods and Applications. *Advances in Water Resources*, 163:104144, May 2022. ISSN 03091708. doi: 10.1016/j.advwatres.2022.104144.
- Abubakar Haruna, Juliette Blanchet, and Anne-Catherine Favre. Modeling Intensity-Duration-Frequency Curves for the Whole Range of Non-Zero Precipitation: A Comparison of Models. *Water Resources Research*, 59(6): e2022WR033362, June 2023. ISSN 0043-1397, 1944-7973. doi: 10.1029/2022WR033362.
- J. R. M. Hosking. L-Moments: Analysis and Estimation of Distributions Using Linear Combinations of Order Statistics. *Journal of the Royal Statistical Society. Series B (Methodological)*, 52(1):105–124, 1990. ISSN 0035-9246.
- J. R. M. Hosking. *Regional Frequency Analysis: An Approach Based on L-moments / J.R.M. Hosking and J.R. Wallis*. Cambridge University Press, Cambridge, United Kingdom, 1997. ISBN 978-0-521-43045-6.
- Wenfeng Hu, Junqiang Yao, Qing He, and Jing Chen. Elevation-Dependent Trends in Precipitation Observed over and around the Tibetan Plateau from 1971 to 2017. *Water*, 13(20):2848, October 2021. ISSN 2073-4441. doi: 10.3390/w13202848.
- Savannah K. Jorgensen and John W. Nielsen-Gammon. Nonstationarity in Extreme Precipitation Return Values Along the United States Gulf and Southeastern Coasts. *Journal of Hydrometeorology*, -1(aop), March 2024. ISSN 1525-7541, 1525-755X. doi: 10.1175/JHM-D-22-0157.1.
- R. W. Kates, C. E. Colten, S. Laska, and S. P. Leatherman. Reconstruction of New Orleans after Hurricane Katrina: A research perspective. *Proceedings of the National Academy of Sciences*, 103(40):14653–14660, October 2006. doi: 10.1073/pnas.0605726103.
- R W Katz, M B Parlange, and P Naveau. Statistics of extremes in hydrology. *Advances in Water Resources*, 25(8-12): 1287–1304, 2002. doi: 10.1016/s0309-1708(02)00056-8.
- Charles D. Keeling, Robert B. Bacastow, Arnold E. Bainbridge, Carl A. Ekdahl, Peter R. Guenther, Lee S. Waterman, and John F. S. Chin. Atmospheric carbon dioxide variations at Mauna Loa Observatory, Hawaii. *Tellus A: Dynamic Meteorology and Oceanography*, 28(6):538, January 1976. ISSN 1600-0870. doi: 10.3402/tellusa.v28i6.11322.
- Roger Koenker and José A. F. Machado. Goodness of Fit and Related Inference Processes for Quantile Regression. *Journal of the American Statistical Association*, 94(448):1296–1310, December 1999. ISSN 0162-1459. doi: 10.1080/01621459.1999.10473882.
- Ioannis M. Kourtis and Vassilios A. Tsihrintzis. Update of intensity-duration-frequency (IDF) curves under climate change: A review. *Water Supply*, 22(5):4951–4974, March 2022. ISSN 1606-9749. doi: 10.2166/ws.2022.152.
- David C. Lafferty and Ryan L. Sriver. Downscaling and bias-correction contribute considerable uncertainty to local climate projections in CMIP6. *npj Climate and Atmospheric Science*, 6(1):1–13, September 2023. ISSN 2397-3722. doi: 10.1038/s41612-023-00486-0.
- Upmanu Lall, Thomas Johnson, Peter Colohan, Amir Aghakouchak, Sankar Arumugam, Casey Brown, Gregory J. McCabe, and Roger S. Pulwarty. *Chapter 3: Water*. U.S. Global Change Research Program, Washington, D.C., 2018. doi: 10.7930/NCA4.2018.CH3.
- Ben Seiyon Lee and Murali Haran. PICAR: An Efficient Extendable Approach for Fitting Hierarchical Spatial Models. *Technometrics*, 64(2):187–198, April 2022. ISSN 0040-1706, 1537-2723. doi: 10.1080/00401706.2021.1933596.
- Carlos H R Lima, Upmanu Lall, Tara Troy, and Naresh Devineni. A hierarchical Bayesian GEV model for improving local and regional flood quantile estimates. *Journal of Hydrology*, 541:816–823, October 2016. doi: 10.1016/j.jhydrol.2016.07.042.
- Tania Lopez-Cantu and Constantine Samaras. Temporal and spatial evaluation of stormwater engineering standards reveals risks and priorities across the United States. *Environmental Research Letters*, 13(7), June 2018. ISSN 1748-9326. doi: 10.1088/1748-9326/aac696.
- Yali Luo, Jiahua Zhang, Miao Yu, Xudong Liang, Rudi Xia, Yanyu Gao, Xiaoyu Gao, and Jinfang Yin. On the Influences of Urbanization on the Extreme Rainfall over Zhengzhou on 20 July 2021: A Convection-Permitting Ensemble Modeling Study. *Advances in Atmospheric Sciences*, 40(3):393–409, March 2023. ISSN 0256-1530, 1861-9533. doi: 10.1007/s00376-022-2048-8.
- Rezaul Mahmood, Roger A. Pielke, Kenneth G. Hubbard, Dev Niyogi, Paul A. Dirmeyer, Clive McAlpine, Andrew M. Carleton, Robert Hale, Samuel Gameda, Adriana Beltrán-Przekurat, Bruce Baker, Richard McNider, David R. Legates, Marshall Shepherd, Jinyang Du, Peter D. Blanken, Oliver W. Frauenfeld, U.S. Nair, and Souleymane Fall. Land cover changes and their biogeophysical effects on climate. *International Journal of Climatology*, 34(4): 929–953, March 2014. ISSN 0899-8418, 1097-0088. doi: 10.1002/joc.3736.

- Jean-Luc Martel, François P. Brissette, Philippe Lucas-Picher, Magali Troin, and Richard Arsenault. Climate Change and Rainfall Intensity–Duration–Frequency Curves: Overview of Science and Guidelines for Adaptation. *Journal of Hydrologic Engineering*, 26(10):03121001, October 2021. ISSN 1084-0699, 1943-5584. doi: 10.1061/(ASCE)HE.1943-5584.0002122.
- Eduardo S. Martins and Jerry R. Stedinger. Generalized maximum-likelihood generalized extreme-value quantile estimators for hydrologic data. *Water Resources Research*, 36(3):737–744, 2000. ISSN 1944-7973. doi: 10.1029/1999WR900330.
- Bruno Merz, Jeroen C J H Aerts, Karsten Arnbjerg-Nielsen, M Baldi, A Becker, A Bichet, Günter Blöschl, Laurens M Bouwer, Achim Brauer, F Cioffi, J M Delgado, M Gocht, F Guzzetti, S Harrigan, K Hirschboeck, C Kilsby, W Kron, H H Kwon, Upmanu Lall, R Merz, K Nissen, P Salvatti, Tina Swierczynski, U Ulbrich, A Viglione, P J Ward, M Weiler, B Wilhelm, and M Nied. Floods and climate: Emerging perspectives for flood risk assessment and management. *Natural Hazards and Earth System Science*, 14(7):1921–1942, 2014. doi: 10/gb9nzm.
- P C D Milly, Julio Betancourt, M Falkenmark, R M Hirsch, Z W Kundzewicz, D P Lettenmaier, and R J Stouffer. Stationarity is dead: Whither water management? *Science*, 319(5863):573–574, February 2008. doi: 10.1126/science.1151915.
- Arianna Miniussi and Marco Marani. Estimation of Daily Rainfall Extremes Through the Metastatistical Extreme Value Distribution: Uncertainty Minimization and Implications for Trend Detection. *Water Resources Research*, 56(7):e2019WR026535, 2020. ISSN 1944-7973. doi: 10.1029/2019WR026535.
- Ashok K. Mishra and Vijay P. Singh. Changes in extreme precipitation in Texas. *Journal of Geophysical Research: Atmospheres*, 115(D14):2009JD013398, July 2010. ISSN 0148-0227. doi: 10.1029/2009JD013398.
- Hamed R. Moftakhari, Amir AghaKouchak, Brett F. Sanders, Maura Allaire, and Richard A. Matthew. What Is Nuisance Flooding? Defining and Monitoring an Emerging Challenge. *Water Resources Research*, 54(7):4218–4227, 2018. ISSN 1944-7973. doi: 10.1029/2018WR022828.
- Alberto Montanari and Demetris Koutsoyiannis. Modeling and mitigating natural hazards: Stationarity is immortal! *Water Resources Research*, 50(12):9748–9756, December 2014. doi: 10.1002/2014wr016092.
- John W. Nielsen-Gammon. Observation-based estimates of present-day and future climate change impacts on heavy rainfall in Harris County. Technical report, June 2020.
- Paul A O’Gorman. Precipitation extremes under climate change. *Current Climate Change Reports*, 1(2):49–59, April 2015. doi: 10.1007/s40641-015-0009-3.
- Álvaro Ossandón, Balaji Rajagopalan, and William Kleiber. Spatial-temporal multivariate semi-Bayesian hierarchical framework for extreme precipitation frequency analysis. *Journal of Hydrology*, 600:126499, September 2021. ISSN 0022-1694. doi: 10.1016/j.jhydrol.2021.126499.
- Angeline G. Pendergrass, Reto Knutti, Flavio Lehner, Clara Deser, and Benjamin M. Sanderson. Precipitation variability increases in a warmer climate. *Scientific Reports*, 7(1):1–9, December 2017. ISSN 2045-2322. doi: 10.1038/s41598-017-17966-y.
- Sanja Perica, Deborah Martin, Sandra Pavlovic, Ishani Roy, Michael St. Laurent, Carl Trypaluk, Dale Unruh, Michael Yekta, and Geoffrey Bonnin. NOAA Atlas 14. Technical Report Volume 9 Version 2.0: Southeastern States (Alabama, Arkansas, Florida, Georgia, Louisiana, Mississippi), National Weather Service, National Oceanic and Atmospheric Administration, U.S. Department of Commerce, Silver Spring, MD, 2013.
- Sanja Perica, Sandra Pavlovic, Michael St. Laurent, Carl Trypaluk, Dale Unruh, and Orlan Wilhite. NOAA Atlas 14. Technical Report Volume 11 Version 2.0: Texas, National Weather Service, National Oceanic and Atmospheric Administration, U.S. Department of Commerce, Silver Spring, MD, 2018.
- R. A. Pielke Sr., J. Adegoke, A. Beltrán-Przekurat, C. A. Hiemstra, J. Lin, U. S. Nair, D. Niyogi, and T. E. Nobis. An overview of regional land-use and land-cover impacts on rainfall. *Tellus B: Chemical and Physical Meteorology*, 59(3):587, January 2007. ISSN 1600-0889, 0280-6509. doi: 10.1111/j.1600-0889.2007.00251.x.
- Elisa Ragno, Amir AghaKouchak, Linyin Cheng, and Mojtaba Sadegh. A generalized framework for process-informed nonstationary extreme value analysis. *Advances in Water Resources*, 130:270–282, August 2019. ISSN 0309-1708. doi: 10.1016/j.advwatres.2019.06.007.
- J. O. Ramsay and B. W. Silverman. *Functional Data Analysis*. Springer Series in Statistics. Springer New York, New York, NY, second edition edition, 2005. ISBN 978-0-387-40080-8. doi: 10.1007/b98888.
- Carl Edward Rasmussen and Chris K I Williams. *Gaussian Processes for Machine Learning*. the MIT Press, 2006. ISBN 0-262-18253-X.

- Mark D. Risser and Michael F. Wehner. Attributable Human-Induced Changes in the Likelihood and Magnitude of the Observed Extreme Precipitation during Hurricane Harvey. *Geophysical Research Letters*, 44(24), December 2017. ISSN 0094-8276, 1944-8007. doi: 10.1002/2017GL075888.
- Bernice R. Rosenzweig, Lauren McPhillips, Heejun Chang, Chingwen Cheng, Claire Welty, Marissa Matsler, David Iwaniec, and Cliff I. Davidson. Pluvial flood risk and opportunities for resilience. *WIREs Water*, 5(6), November 2018. ISSN 2049-1948, 2049-1948. doi: 10.1002/wat2.1302.
- Mauro Rubino, David Etheridge, David Thornton, Colin Allison, Roger Francey, Ray Langenfelds, Paul Steele, Cathy Trudinger, Darren Spencer, Mark Curran, Tas Van Ommen, and Andrew Smith. Law Dome Ice Core 2000-Year CO₂, CH₄, N₂O and d13C-CO₂, 2019.
- Brook T. Russell, Mark D. Risser, Richard L. Smith, and Kenneth E. Kunkel. Investigating the association between late spring Gulf of Mexico sea surface temperatures and U.S. Gulf Coast precipitation extremes with focus on Hurricane Harvey. *Environmetrics*, 31(2):e2595, 2020. ISSN 1099-095X. doi: 10.1002/env.2595.
- J D Salas, J Obeysekera, and R M Vogel. Techniques for assessing water infrastructure for nonstationary extreme events: A review. *Hydrological Sciences Journal*, 63(3):325–352, 2018. doi: 10.1080/02626667.2018.1426858.
- Katherine E. Schlef, Kenneth E. Kunkel, Casey Brown, Yonas Demissie, Dennis P. Lettenmaier, Anna Wagner, Mark S. Wigmosta, Thomas R. Karl, David R. Easterling, Kimberly J. Wang, Baptiste François, and Eugene Yan. Incorporating non-stationarity from climate change into rainfall frequency and intensity-duration-frequency (IDF) curves. *Journal of Hydrology*, 616:128757, January 2023. ISSN 0022-1694. doi: 10.1016/j.jhydrol.2022.128757.
- Alexandra M. Schmidt and Alan E. Gelfand. A Bayesian coregionalization approach for multivariate pollutant data. *Journal of Geophysical Research: Atmospheres*, 108(D24):2002JD002905, December 2003. ISSN 0148-0227. doi: 10.1029/2002JD002905.
- Reinhard Selten. Axiomatic Characterization of the Quadratic Scoring Rule. *Experimental Economics*, 1(1):43–61, June 1998. ISSN 1573-6938. doi: 10.1023/A:1009957816843.
- S.I. Seneviratne, X. Zhang, M. Adnan, W. Badi, C. Dereczynski, A. Di Luca, S. Ghosh, I. Iskandar, J. Kossin, S. Lewis, F. Otto, I. Pinto, M. Satoh, S.M. Vicente-Serrano, M. Wehner, and B. Zhou. Weather and climate extreme events in a changing climate. In V. Masson-Delmotte, P. Zhai, A. Pirani, S. L. Connors, C. Péan, S. Berger, N. Caud, Y. Chen, L. Goldfarb, M. I. Gomis, M. Huang, K. Leitzell, E. Lonnoy, J. B. R. Matthews, T. K. Maycock, T. Waterfield, O. Yelekçi, R. Yu, and B. Zhou, editors, *Climate Change 2021: The Physical Science Basis. Contribution of Working Group I to the Sixth Assessment Report of the Intergovernmental Panel on Climate Change*, book section 11. Cambridge University Press, Cambridge, UK and New York, NY, USA, 2021. doi: 10.1017/9781009157896.013.
- Francesco Serinaldi and Chris G Kilsby. Stationarity is undead: Uncertainty dominates the distribution of extremes. *Advances in Water Resources*, 77:17–36, March 2015. doi: 10.1016/j.advwatres.2014.12.013.
- Sanjib Sharma, Ben Seiyon Lee, Robert E. Nicholas, and Klaus Keller. A Safety Factor Approach to Designing Urban Infrastructure for Dynamic Conditions. *Earth's Future*, 9(12):e2021EF002118, 2021. ISSN 2328-4277. doi: 10.1029/2021EF002118.
- Daniele Feitoza Silva, Slobodan P. Simonovic, Andre Schardong, and Joel Avruch Goldenfum. Assessment of non-stationary IDF curves under a changing climate: Case study of different climatic zones in Canada. *Journal of Hydrology: Regional Studies*, 36:100870, August 2021. ISSN 2214-5818. doi: 10.1016/j.ejrh.2021.100870.
- Adam H. Sobel, Chia-Ying Lee, Steven G. Bowen, Suzana J. Camargo, Mark A. Cane, Amy Clement, Boniface Fosu, Megan Hart, Kevin A. Reed, Richard Seager, and Michael K. Tippett. Near-term tropical cyclone risk and coupled Earth system model biases. *Proceedings of the National Academy of Sciences*, 120(33):e2209631120, August 2023. doi: 10.1073/pnas.2209631120.
- Xiaomeng Song, Xianju Zou, Yuchen Mo, Jianyun Zhang, Chunhua Zhang, and Yimin Tian. Nonstationary bayesian modeling of precipitation extremes in the Beijing-Tianjin-Hebei Region, China. *Atmospheric Research*, 242: 105006, September 2020. ISSN 0169-8095. doi: 10.1016/j.atmosres.2020.105006.
- Stan Development Team. *Stan User's Guide*. Version 2.30 edition, 2022.
- Madeline D. Statkewicz, Robert Talbot, and Bernhard Rappenglueck. Changes in precipitation patterns in Houston, Texas. *Environmental Advances*, 5:100073, October 2021. ISSN 2666-7657. doi: 10.1016/j.envadv.2021.100073.
- Jery R. Stedinger. Expected probability and annual damage estimators. *Journal of Water Resources Planning and Management*, 123(2):125–135, March 1997. ISSN 0733-9496. doi: 10.1061/(ASCE)0733-9496(1997)123:2(125).
- Alec G. Stephenson, Eric A. Lehmann, and Alope Phatak. A max-stable process model for rainfall extremes at different accumulation durations. *Weather and Climate Extremes*, 13:44–53, September 2016. ISSN 22120947. doi: 10.1016/j.wace.2016.07.002.

- Xinxin Sui, Zong-Liang Yang, Marshall Shepherd, and Dev Niyogi. Global scale assessment of urban precipitation anomalies. *Proceedings of the National Academy of Sciences*, 121(38):e2311496121, September 2024. doi: 10.1073/pnas.2311496121.
- Jianhua Sun, Shenming Fu, Huijie Wang, Yuanchun Zhang, Yun Chen, Aifang Su, Yaqiang Wang, Huan Tang, and Ruoyun Ma. Primary characteristics of the extreme heavy rainfall event over Henan in July 2021. *Atmospheric Science Letters*, 24(1):e1131, 2023. ISSN 1530-261X. doi: 10.1002/asl.1131.
- Qiaohong Sun, Xuebin Zhang, Francis Zwiers, Seth Westra, and Lisa V. Alexander. A Global, Continental, and Regional Analysis of Changes in Extreme Precipitation. *Journal of Climate*, 34(1):243–258, January 2021. ISSN 0894-8755, 1520-0442. doi: 10.1175/JCLI-D-19-0892.1.
- Rocky Talchabhadel, Ramchandra Karki, Bhesh Raj Thapa, Manisha Maharjan, and Binod Parajuli. Spatio-temporal variability of extreme precipitation in Nepal. *International Journal of Climatology*, 38(11):4296–4313, September 2018. ISSN 0899-8418, 1097-0088. doi: 10.1002/joc.5669.
- Marco Tedesco, Steven McAlpine, and Jeremy R. Porter. Exposure of real estate properties to the 2018 Hurricane Florence flooding. *Natural Hazards and Earth System Sciences*, 20(3):907–920, April 2020. ISSN 1561-8633. doi: 10.5194/nhess-20-907-2020.
- The Federal Emergency Management Agency. Guidance for flood risk analysis and mapping: Hydrology rainfall-runoff analysis. Guidance Document 91, 2019.
- M. Thiemann, M. Trosset, H. Gupta, and S. Sorooshian. Bayesian recursive parameter estimation for hydrologic models. *Water Resources Research*, 37(10):2521–2535, 2001. ISSN 1944-7973. doi: 10.1029/2000WR900405.
- Jana Ulrich, Oscar E. Jurado, Madlen Peter, Marc Scheibel, and Henning W. Rust. Estimating IDF Curves Consistently over Durations with Spatial Covariates. *Water*, 12(11):3119, November 2020. ISSN 2073-4441. doi: 10.3390/w12113119.
- Karin van der Wiel, Sarah B. Kapnick, Geert Jan van Oldenborgh, Kirien Whan, Sjoukje Philip, Gabriel A. Vecchi, Roop K. Singh, Julie Arrighi, and Heidi Cullen. Rapid attribution of the August 2016 flood-inducing extreme precipitation in south Louisiana to climate change. *Hydrology and Earth System Sciences*, 21(2):897–921, February 2017. ISSN 1027-5606. doi: 10.5194/hess-21-897-2017.
- Geert Jan van Oldenborgh, Karin van der Wiel, Antonia Sebastian, Roop Singh, Julie Arrighi, Friederike Otto, Karsten Haustein, Sihan Li, Gabriel Vecchi, and Heidi Cullen. Attribution of extreme rainfall from Hurricane Harvey, August 2017. *Environmental Research Letters*, 12(12):124009, December 2017. ISSN 1748-9326. doi: 10.1088/1748-9326/aa9ef2.
- Christopher K. Wikle. Comparison of Deep Neural Networks and Deep Hierarchical Models for Spatio-Temporal Data. *arXiv:1902.08321 [cs, stat]*, February 2019.
- Daniel B. Wright, Guo Yu, and John F. England. Six decades of rainfall and flood frequency analysis using stochastic storm transposition: Review, progress, and prospects. *Journal of Hydrology*, 585:124816, June 2020. ISSN 0022-1694. doi: 10.1016/j.jhydrol.2020.124816.
- Wei Zhang, Gabriele Villarini, Gabriel A. Vecchi, and James A. Smith. Urbanization exacerbated the rainfall and flooding caused by hurricane Harvey in Houston. *Nature*, 563(7731):384–388, November 2018. ISSN 1476-4687. doi: 10.1038/s41586-018-0676-z.

A Supplement figures

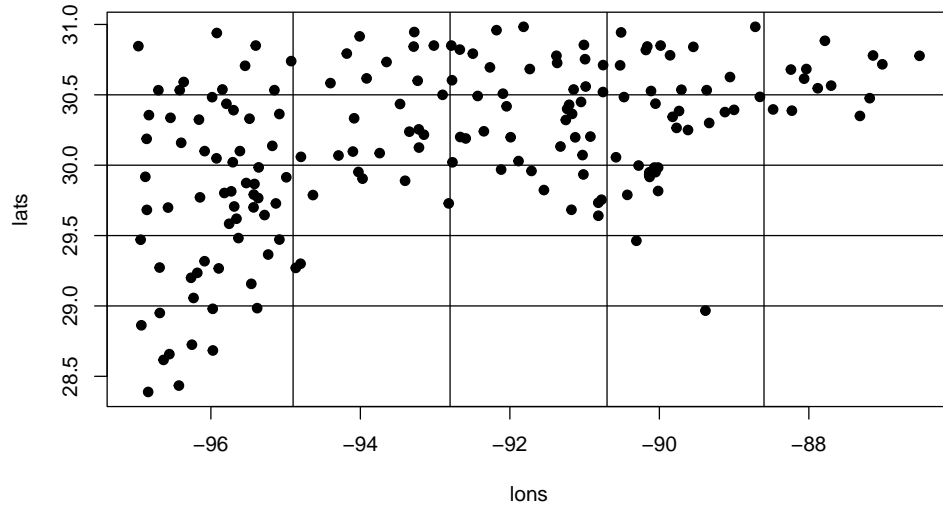


Figure A1: The study area is divided into 25 grids, which are utilized to create cross-validation subsets.

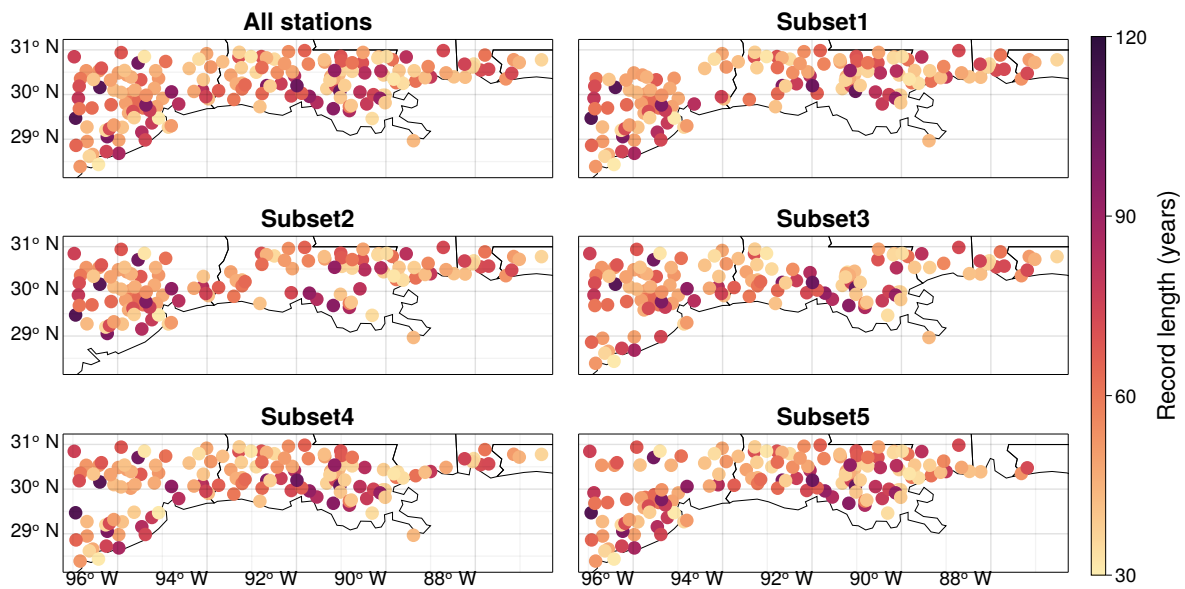


Figure A2: Maps show the full dataset and station subsets used for cross-validation along with the record length for each station.

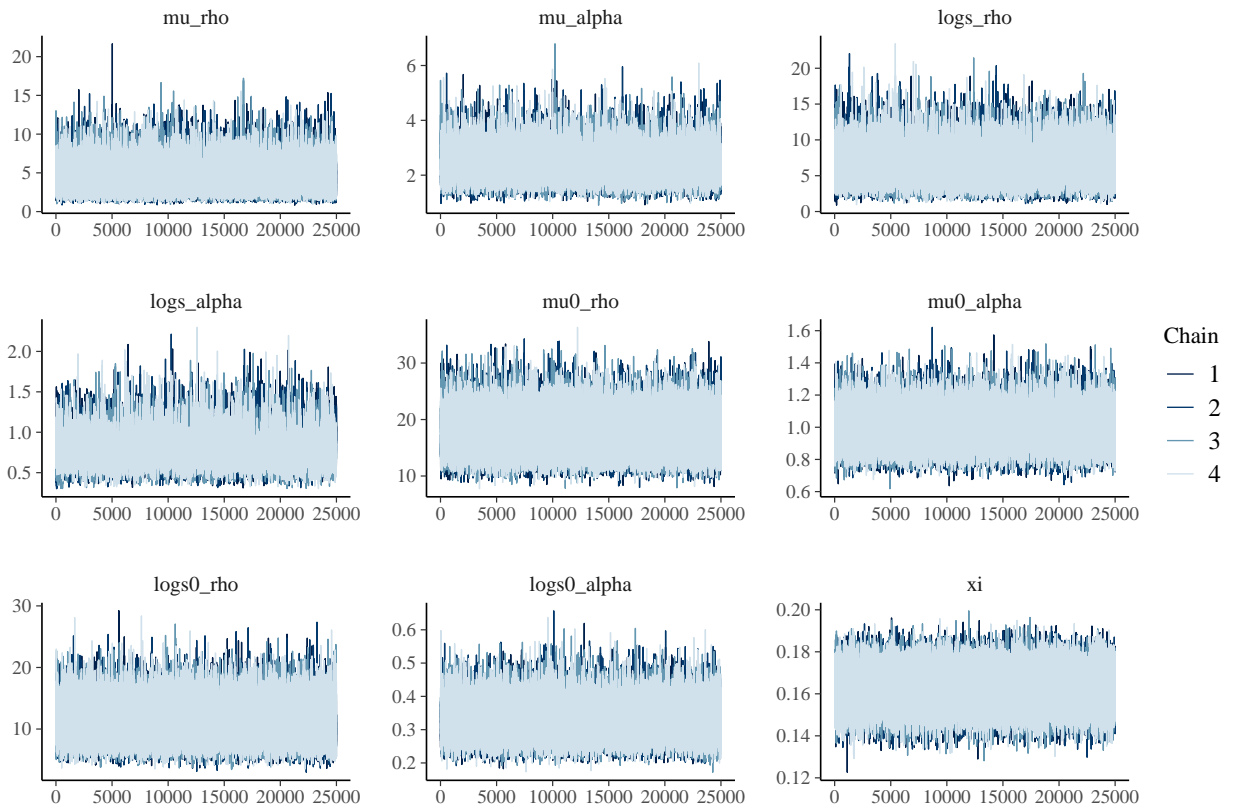


Figure A3: Trace plots indicate generally good posterior convergence. We present the trace plots for the key parameters obtained from MCMC simulations using the full dataset.

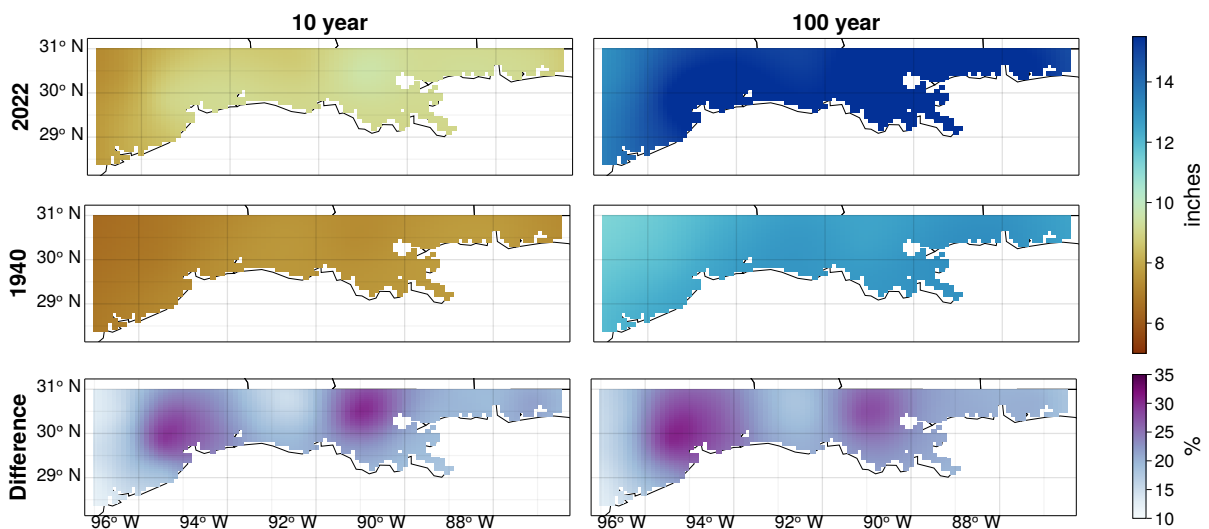


Figure A4: Similar to fig. 7, this figure presents the results in a gridded format. It displays the gridded posterior mean of extreme precipitation return level estimates for the (L) 10-year and (R) 100-year events. The estimates are shown for (T) 2022, (M) 1940, and (B) the percentage change from 1940 to 2022. These results are obtained using the Spatially Varying Covariates Model, where distribution parameters are interpolated with GP.